PHYSICAL REVIEW A **88**, 033852 (2013)

Quantum limits on probabilistic amplifiers

Shashank Pandey,[1] Zhang Jiang,[1] Joshua Combes,[1] and Carlton M. Caves[1,2,*]

[1]*Center for Quantum Information and Control, University of New Mexico, Albuquerque, New Mexico 87131-0001, USA*

[2]*Centre for Engineered Quantum Systems, School of Mathematics and Physics, University of Queensland, Brisbane, Queensland 4072, Australia*

(Received 29 May 2013; published 30 September 2013)

An ideal phase-preserving linear amplifier is a deterministic device that adds to an input signal the minimal amount of noise consistent with the constraints imposed by quantum mechanics. A noiseless linear amplifier takes an input coherent state to an amplified coherent state, but only works part of the time. Such a device is actually better than noiseless, since the output has less noise than the amplified noise of the input coherent state; for this reason we refer to such devices as *immaculate*. Here we bound the working probabilities of probabilistic and approximate immaculate amplifiers and construct theoretical models that achieve some of these bounds. Our chief conclusions are the following: (i) The working probability of any phase-insensitive immaculate amplifier is very small in the phase-plane region where the device works with high fidelity; (ii) phase-sensitive immaculate amplifiers that work only on coherent states sparsely distributed on a phase-plane circle centered at the origin can have a reasonably high working probability.

DOI: 10.1103/PhysRevA.88.033852 PACS number(s): 42.65.Yj, 03.67.−a, 42.50.Lc

I. INTRODUCTION AND MOTIVATION

Classical noninverting amplifiers take a macroscopic input signal, such as a time-varying voltage, and produce an output signal that is a rescaled version of the input signal. The ratio of the input amplitude to the output amplitude is called the gain g of the amplifier. Classical amplifiers are used ubiquitously, e.g., to boost signal strength for classical communications or to increase the power of signals driving loudspeakers. In principle, a classical amplifier can be noise free in the sense that no noise is added to the input signal. The only truly fundamental limit on amplification comes from quantum mechanics.

The canonical quantum amplifier is called a phase-preserving linear quantum amplifier. It takes an input bosonic signal and produces a larger output signal [1–3], while preserving the phase. The quantum constraints on the operation of such a device are ultimately a consequence of unitarity and can be thought as coming from the prohibition on transformations that increase the distinguishability of nonorthogonal states [4,5]. The quantum constraint on a high-gain device can be expressed as the requirement that the amplifier must add noise that, when referred to the input, is at least as big as an extra unit of vacuum noise. A device that achieves the minimal added noise is called an *ideal* linear amplifier.

To understand the purpose of quantum amplifiers, it is instructive to look at how they are used. An illustrative case involves experiments probing quantum mechanics at microwave frequencies. Experimenters wish to measure the small amplitude and phase shifts of a field that is used to probe another quantum system. It turns out that quantum-limited simultaneous measurements of both amplitude and phase shifts introduce the same additional unit of vacuum noise as does an ideal linear amplifier [6]. Thus, in principle, measuring at the input or amplifying and measuring at the output both provide the same signal-to-noise ratio (SNR); the practical question becomes whether it is easier to do quantum-limited measurement or to do quantum-limited amplification and subsequent measurement at the output. The answer at microwave frequencies is that amplifiers operate closer to quantum limits.

Recently, Ralph and Lund [7] proposed a device, which they call a "nondeterministic noiseless linear amplifier," previously considered by Fiurášek [8] in the context of probabilistic cloning. The idea behind the Ralph-Lund device is that it might be possible to *improve* the SNR in some number of trials or experiments, while the device fails in the remaining runs. Specifically, what Ralph and Lund proposed is a device that takes an input coherent state $|\alpha\rangle$ to a target coherent state $|g\alpha\rangle$ with (success) probability $p_{\checkmark}$ and fails with probability $1-p_{\checkmark}$. Such a device is even better than noiseless, because when the output noise is referred to the input, it is smaller than the original coherent-state noise by a factor of $1/g^2$. In particular, it is better than a device that amplifies the input noise to the output without the addition of any noise, a device that we call a *perfect amplifier*. Because it is better than perfect, we call Ralph and Lund's proposal an *immaculate amplifier*. The purpose of this paper is to analyze in detail and to bound the performance of immaculate linear amplifiers.

In Sec. II we review recent work on deterministic linear amplifiers [3], which allows us to consider on the same footing ideal linear amplifiers and (unphysical) perfect and immaculate amplifiers. We use this discussion to motivate the idea of nondeterministic, or probabilistic, versions of perfect and immaculate amplifiers, and we use a simple uncertainty-principle argument to bound the working probability of probabilistic perfect and immaculate amplifiers.

Section III reviews the relation between amplification and cloning, thus connecting the results in this paper to the literature on cloning of coherent states, and Sec. IV reviews proposals for and experimental implementations of immaculate linear amplifiers.

Sections V and VI are the heart of the paper, the place where we derive bounds on the operation of immaculate amplifiers.

*ccaves@unm.edu

Immaculate amplifiers that produce the target coherent state exactly, but are allowed to fail, are the subject of Sec. V; they are closely related to unambiguous state discrimination [9,10], in which one discriminates among a set of linearly independent states exactly, but can declare a failure to discriminate. We use results from unambiguous state discrimination to bound the working probability of an immaculate amplifier that amplifies M coherent states uniformly spaced around a circle of radius $|\alpha|$ centered at the origin of the phase plane. In the case of many coherent states on both the input and the output circles, i.e., assuming $M \gg g^2|\alpha|^2$, the working probability is bounded by

$$p_{\checkmark} \leqslant \frac{e^{(g^2-1)|\alpha|^2}}{g^{2(M-1)}} \ll \left(\frac{\sqrt{e}}{g^2}\right)^{2(M-1)}. \tag{1.1}$$

This success probability decreases exponentially with M and goes to zero in the phase-insensitive limit $M \to \infty$. We stress that this means that an immaculate amplifier that works exactly on an entire circle of input coherent states never works.

For an immaculate amplifier that acts on all coherent states on M equally spaced spokes of a disk of any radius $|\alpha| > 0$ centered at the origin, the success probability is governed by the limiting circle of zero radius and thus is bounded by

$$p_{\checkmark} \leqslant \frac{1}{g^{2(M-1)}} \tag{1.2}$$

for any $M \geqslant 2$. This success probability goes to zero in the phase-insensitive limit $M \to \infty$.

On a more optimistic note, we also show in Sec. V that if the M coherent states are more than about a vacuum unit apart on the input circle, they can be immaculately amplified with a success probability exceeding a half. This suggests that practical applications of immaculate amplifiers are likely to be as amplifiers that are both phase sensitive and amplitude specific in that they only work well on a discrete set of states on a particular phase-plane circle. Such an amplitude-specific, phase-sensitive amplifier might prove useful, for example, in discriminating the coherent states used in phase-shift keying [11,12].

The results of Sec. V indicate that exact immaculate amplification and phase insensitivity do not go well together. In Sec. VI we explore this incompatibility further by dropping exactness and investigating the performance of approximate, probabilistic immaculate amplifiers that are explicitly phase insensitive. We characterize such a device by its amplitude gain and by the radius $\sqrt{N}/g$ of the disk, centered at the origin, over which it amplifies an input coherent $|\alpha\rangle$ to the target output state $|g\alpha\rangle$ with near unit fidelity. The high-fidelity outputs thus lie within a disk of radius $\sqrt{N}$. By finding the optimal such amplifier, we show that the best success probability in the high-fidelity input region is

$$p_{\checkmark} = \frac{e^{-|\alpha|^2}}{g^{2N}}, \quad |\alpha|^2 \lesssim N/g^2, \tag{1.3}$$

which decreases exponentially with N. We use our results to investigate the performance of phase-insensitive immaculate amplifiers within the context of the SNRs for measurements of amplitude and phase shifts discussed above.

Because the success probability (1.3) is so small, we suggest that a good performance measure for phase-insensitive immaculate amplifiers must include both the fidelity with the target output $|g\alpha\rangle$ and the success probability. A natural combination is the product of the two, which can be thought of as the overall probability to reach the target. We show that over the whole range of operation of the optimal phase-insensitive immaculate amplifier, this probability-fidelity product is never better than that of the identity operation. This can be summarized by saying that in terms of the probability-fidelity product, *phase-preserving* immaculate amplification is never better than doing nothing, thus reenforcing our conclusion that any practical application of immaculate amplification lies in phase-sensitive amplification.

A concluding Sec. VII wraps up by summarizing our key results and discussing avenues along which future research might and should proceed.

II. PHYSICAL AND UNPHYSICAL LINEAR AMPLIFIERS

A. Context

The setting for our investigation is a signal carried by a single-mode field,

$$E(t) = \frac{1}{2}(ae^{-i\omega t} + a^\dagger e^{-i\omega t}) = \frac{1}{\sqrt{2}}(x_1 \cos\omega t + x_2 \sin\omega t). \tag{2.1}$$

This *primary mode*, which we label by A, is to undergo phase-preserving linear amplification. The annihilation and creation operators, a and $a^\dagger$, are related to the Hermitian quadrature components, x_1 and x_2, by $a = (x_1 + ix_2)/\sqrt{2}$, $a^\dagger = (x_1 - ix_2)/\sqrt{2}$, where $[a,a^\dagger] = 1$ or, equivalently, $[x_1,x_2] = i$.

The annihilation operator is a complex-amplitude operator for the field, measured in photon-number units; the expectation value of the field, $\langle E(t)\rangle = \mathrm{Re}(\langle a\rangle e^{-i\omega t})$, oscillates with the amplitude and phase of $\langle a\rangle$. The variance of E characterizes the noise in the signal; for phase-insensitive noise, for which $\langle(\Delta a)^2\rangle = 0$ (we use $\Delta O = O - \langle O\rangle$ here and throughout), this variance is constant in time and given by

$$2\langle(\Delta E)^2\rangle = \langle|\Delta a|^2\rangle = \tfrac{1}{2}\langle \Delta x_1^2 + \Delta x_2^2\rangle \geqslant \tfrac{1}{2}. \tag{2.2}$$

Here $\langle|\Delta a|^2\rangle \equiv \frac{1}{2}\langle \Delta a \Delta a^\dagger + \Delta a^\dagger \Delta a\rangle$ is the symmetrically ordered second moment of a. The inequality follows directly from the uncertainty principle for the quadrature components, $\langle(\Delta x_1)^2\rangle\langle(\Delta x_2)^2\rangle \geqslant 1/4$. The lower bound is the half-quantum of zero-point (or vacuum) noise and is saturated if and only if the mode is in a coherent state $|\alpha\rangle$.

The objective of phase-preserving linear amplification is to increase the size of the input signal by a (real) amplitude gain g, regardless of the input phase, while introducing as little noise as possible. The amplification of the input signal can be expressed as a transformation of the expected complex amplitude,

$$\langle a_{\mathrm{out}}\rangle = g\langle a_{\mathrm{in}}\rangle. \tag{2.3}$$

A *perfect linear amplifier* would perform this feat while adding no noise; in the Heisenberg picture, the primary mode's annihilation operator, not just its expectation value, would transform from input to output as

$$a_{\mathrm{out}} = g a_{\mathrm{in}}. \tag{2.4}$$

The second-moment noise would be amplified by the power gain g^2, i.e., $\langle|\Delta a_{\rm out}|^2\rangle = g^2\langle|\Delta a_{\rm in}|^2\rangle$. The amplifier's output would be contaminated by the same noise as the input, blown up by a factor of g^2, but the amplification process would not add any noise to the amplified input noise.

There are, however, no perfect phase-preserving linear amplifiers; the transformation (2.4) does not preserve the canonical commutation relation and thus violates unitarity. Physically, this is the statement that amplification of the primary mode requires it to be coupled to other physical systems, not least to provide the energy needed for amplification; these other systems, which can be thought of as the amplifier's internal degrees of freedom, necessarily add noise to the output. This physical requirement is expressed in an input-output relation [1,2],

$$a_{\rm out} = g a_{\rm in} + L^\dagger, \tag{2.5}$$

where the *added-noise operator* L is a property of the internal degrees of freedom. One usually assumes that $\langle L^\dagger\rangle = 0$ so as to retain the expectation-value transformation (2.3). Preserving the canonical commutation relation between input and output requires that

$$[L, L^\dagger] = g^2 - 1, \tag{2.6}$$

which implies an uncertainty principle for the added noise,

$$\langle|\Delta L|^2\rangle \geqslant \tfrac{1}{2}(g^2 - 1). \tag{2.7}$$

The amplifier must be prepared to receive any input in the primary mode, without having any idea what that input is going to be. This places the restriction that the primary mode and the internal degrees of freedom *cannot* be correlated before amplification. The total output noise is then the sum of the amplified input noise and the noise added by the internal degrees of freedom:

$$\langle|\Delta a_{\rm out}|^2\rangle = g^2\langle|\Delta a_{\rm in}|^2\rangle + \langle|\Delta L|^2\rangle \geqslant g^2 - \tfrac{1}{2}. \tag{2.8}$$

The lower bound follows from the uncertainty principles (2.2) and (2.7). An amplifier that achieves the lower bound in Eq. (2.7), thus adding the least amount of noise permitted by quantum mechanics, is called an *ideal linear amplifier*.

B. Ideal, perfect, and immaculate linear amplifiers

We can formulate a more general description of linear amplifiers by using the formalism developed in Ref. [3], where we showed that for any phase-preserving linear amplifier, its action on an input state ρ of the primary mode can be represented by an amplifier map,

$$\rho_{\rm out} = \mathcal{E}(\rho) = {\rm Tr}_B[S(r)\rho\otimes\sigma S^\dagger(r)]. \tag{2.9}$$

In this expression, σ is the input state of a (perhaps fictitious) ancillary mode B, which has annihilation and creation operators b and $b^\dagger$, and $S(r) = e^{r(ab - a^\dagger b^\dagger)}$ is the two-mode squeeze operator. The amplitude gain is given by $g = \cosh r$, and the noise properties of the amplifier are encoded in σ. The main result of Ref. [3] is that the amplifier map is physical, i.e., is completely positive, if and only if σ is a physical ancilla state.

The P function of the output state can be written as a convolution of the P function of the input state with the Q distribution of σ:

$$P_{\rm out}(\beta) = \int d^2\alpha\, \frac{Q_\sigma[-(\beta^* - g\alpha^*)/\sqrt{g^2-1}\,]}{g^2-1} P_{\rm in}(\alpha). \tag{2.10}$$

We specialize for the remainder of this section to a coherent-state input $|\alpha\rangle$, for which the input P function is a δ distribution and the output P function is obtained by displacing and rescaling the Q distribution of σ,

$$P_{\rm out}(\beta) = \frac{Q_\sigma[-(\beta^* - g\alpha^*)/\sqrt{g^2-1}\,]}{g^2-1}. \tag{2.11}$$

Moments of α calculated using the P function give normally ordered moments of a and $a^\dagger$.

An ideal linear amplifier corresponds uniquely to the case where the input ancilla state is vacuum, i.e., $\sigma = |0\rangle\langle 0|$, giving rise to an output P function,

$$P_{\rm out}(\beta) = \frac{e^{-|\beta - g\alpha|^2/(g^2-1)}}{\pi(g^2-1)}. \tag{2.12}$$

The displacement of the Q distribution indicates that the input complex amplitude is amplified as in Eq. (2.3), and the rescaling of the Q distribution confirms that the total (symmetric) output noise is $\langle|\Delta a_{\rm out}|^2\rangle = \langle\Delta a_{\rm out}^\dagger \Delta a_{\rm out}\rangle + \frac{1}{2} = g^2 - \frac{1}{2}$.

We can embed the ideal-amplifier map in a sequence of maps for both physical and unphysical amplifiers by considering ancilla states of thermal form,

$$\sigma = \frac{1}{\mu^2}\left(1 - \frac{1}{\mu^2}\right)^{a^\dagger a} = \frac{1}{\mu^2}\sum_{n=0}^{\infty}\left(1 - \frac{1}{\mu^2}\right)^n |n\rangle\langle n|. \tag{2.13}$$

When $\mu^2 \in [1,\infty)$, σ is a physical thermal state, with dimensionless inverse temperature β given by $\mu^2 = (1 - e^{-\beta})^{-1}$; $\mu^2 = 1$ gives the vacuum state. When $\mu^2 \in [0,1)$, however, σ has negative eigenvalues and thus is unphysical. When $\mu^2 \in (\frac{1}{2},\infty)$, the trace of σ is well defined and equal to 1, but when $\mu^2 \in [0,1/2]$, the series for the trace of σ diverges; $\mu^2 = 1/2$ makes σ the parity operator. The amplifier maps corresponding to unphysical σ are not completely positive and thus are unphysical [3]. In the following, we sometimes use quotes to warn the reader that σ might not be physical.

The Q function for σ, $Q_\sigma(\alpha) = e^{-|\alpha|^2/\mu^2}/\pi\mu^2$, is well behaved on the entire range $\mu^2 \in (0,\infty)$ and becomes a δ function when $\mu^2 = 0$. The output P function is the Gaussian

$$P_{\rm out}(\beta,\mu^2) = \frac{1}{\pi\mu^2(g^2-1)} e^{-|\beta - g\alpha|^2/\mu^2(g^2-1)}, \tag{2.14}$$

which has normally ordered output noise $\langle\Delta a^\dagger \Delta a\rangle = \mu^2(g^2 - 1)$ and, hence, symmetrically ordered output noise [13],

$$\langle|\Delta a_{\rm out}|^2\rangle = \langle\Delta a_{\rm out}^\dagger \Delta a_{\rm out}\rangle + \tfrac{1}{2} = \mu^2(g^2-1) + \tfrac{1}{2}. \tag{2.15}$$

The output Q distribution is

$$Q_{\rm out}(\beta,\mu^2) = \frac{1}{\pi[\mu^2(g^2-1)+1]} e^{-|\beta - g\alpha|^2/[\mu^2(g^2-1)+1]}. \tag{2.16}$$

We now focus on three amplifiers of interest, which correspond to three values of μ^2:

(1) the *ideal linear amplifier* (physical), which corresponds to $\mu^2 = 1$ and which adds the minimal amount of (symmetrically ordered) noise permitted by quantum mechanics;

(2) the *perfect linear amplifier* (unphysical), $\mu^2 = 1/2$, whose (symmetrically ordered) output noise consists only of the amplified input noise;

(3) the unphysical $\mu^2 = 0$ amplifier, which we christen the *immaculate linear amplifier*, because it is better than perfect, and which takes an input coherent state $|\alpha\rangle$ to an amplified output coherent state $|g\alpha\rangle$; we let $\mathcal{A}$ denote the amplifier map (2.9) for the case of an immaculate linear amplifier, i.e.,

$$\mathcal{A}(|\alpha\rangle\langle\alpha|) = |g\alpha\rangle\langle g\alpha|. \tag{2.17}$$

The operation of these three amplifiers can be understood intuitively in terms of how the output noise arises from amplified input noise and added noise. The three canonical quasidistributions, the P function, the Wigner W function, and the Husimi Q distribution [14], with their different operator orderings, quantify the noise differently and thus provide three different perspectives on the relation between input and output noise. In Fig. 1 we illustrate the amplification transformations for ideal, perfect, and immaculate amplifiers. The transformations can be summarized in terms of ball-and-stick phase-space diagrams that depict the input and output noise as circles of uncertainty centered at the input and output mean complex amplitudes. We give such diagrams for the normally ordered variances corresponding to input and output P functions, as in Eq. (2.14), and also for the symmetrically ordered moments of input and output Wigner W functions and the antinormally ordered moments of input and output Husimi Q distributions.

The P-function perspective, with its normally ordered moments, is matched to the immaculate amplifier map (2.17). The immaculate amplifier takes an input coherent state to an amplified coherent state; in the P-function depiction, it takes an input dot in the phase plane to an output dot, without adding any noise. All the output noise for a perfect or an ideal amplifier appears to be added noise.

The symmetrically ordered moments of the Wigner function give the traditional perspective on amplifier noise. A perfect amplifier amplifies input coherent-state noise without adding any noise. An ideal amplifier adds further noise $\langle|\Delta L|^2\rangle = \frac{1}{2}(g^2 - 1)$, and an immaculate amplifier subtracts the same amount of noise.

The antinormally ordered moments of the Q function give a picture matched to an ideal amplifier. The input noise of a coherent state is amplified by an ideal amplifier to produce the output noise without addition of any further noise. A perfect amplifier has less output noise by $\frac{1}{2}(g^2 - 1)$, and an immaculate amplifier has less noise by $g^2 - 1$.

C. Naive uncertainty-principle bounds on probabilistic μ^2 amplifiers

The antinormally ordered noise of the Q function has a physical interpretation that sheds light on the performance of linear amplifiers. Suppose one wishes to determine the center of a coherent state by making simultaneous measurements of the two quadrature components. The statistics of ideal simultaneous measurements are given by the Q distribution [6], so in ν such measurements, one can determine the

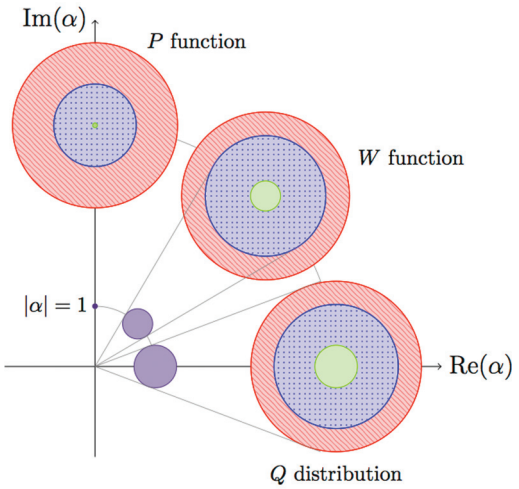

FIG. 1. (Color online) Ball-and-stick phase-space depictions of input and output noise for ideal ($\mu^2 = 1$), perfect ($\mu^2 = \frac{1}{2}$), and immaculate ($\mu^2 = 0$) amplifiers defined by the amplifier map (2.9) with initial ancilla "state" (2.13). Color and fill conventions: Solid (purple) fill is used for input noise; (red) fill with slanted lines for the output noise of an ideal amplifier; (blue) fill with dots for the output of a perfect amplifier; and solid (green) fill for the output of an immaculate amplifier. The primary-mode input is a coherent state $|\alpha\rangle$ with $|\alpha| = 1$, and the gain is $g = 4$, giving the output state a mean that lies on a circle of radius $g|\alpha| = 4$. The input and output states are represented by noise circles centered at the mean complex amplitude (the stick) and having radius $\Sigma/2\sqrt{2}$ (the ball), where $\Sigma^2 = \langle|\Delta\alpha|^2\rangle$ is the variance of the complex amplitude calculated from the appropriate quasidistribution: for the normal ordering of the P function, $\Sigma_P^2 = \langle\Delta a^\dagger \Delta a\rangle$; for the symmetric ordering of the Wigner W function, $\Sigma_W^2 = \frac{1}{2}(\langle\Delta a^\dagger \Delta a\rangle + \langle\Delta a \Delta a^\dagger\rangle) = \Sigma_P^2 + \frac{1}{2}$; for the antinormal ordering of the Q distribution, $\Sigma_Q^2 = \langle\Delta a \Delta a^\dagger\rangle = \Sigma_W^2 + \frac{1}{2}$. The P-function depiction is the one suggested by the amplifier map (2.9): The dot ($\Sigma_P = 0$) for the input coherent state $|\alpha\rangle$ is amplified by an immaculate amplifier to a dot for the output coherent state $|g\alpha\rangle$; the output for a perfect amplifier has additional noise $\Sigma_P^2 = \frac{1}{2}(g^2 - 1)$, and the output for an ideal amplifier has additional noise $\Sigma_P^2 = g^2 - 1$. The symmetrically ordered moments of the Wigner W function give the traditional picture of amplifier noise: the input coherent state, represented by a circle corresponding to $\Sigma_W^2 = \frac{1}{2}$, has its noise amplified by a perfect amplifier along the (gray) radial lines to the circle with $\Sigma_W^2 = \frac{1}{2}g^2$; the output of an ideal amplifier has additional noise $\frac{1}{2}(g^2 - 1)$, giving total noise $\Sigma_W^2 = g^2 - \frac{1}{2}$, and the output of an immaculate amplifier has its noise reduced by $\frac{1}{2}(g^2 - 1)$ to the coherent-state value $\Sigma_W^2 = \frac{1}{2}$. The antinormally ordered moments of the Husimi Q distribution give a picture suited to discussion of simultaneous measurements of the quadrature components (see text): The input coherent state, represented by a circle corresponding to $\Sigma_Q^2 = 1$, has its noise amplified by an ideal amplifier along the (gray) radial lines to a circle with $\Sigma_Q^2 = g^2$; the output of a perfect amplifier has less noise by $\frac{1}{2}(g^2 - 1)$, giving total noise $\Sigma_Q^2 = \frac{1}{2}(g^2 + 1)$, and the output of an immaculate amplifier has its noise reduced by $g^2 - 1$ to the coherent-state value $\Sigma_Q^2 = 1$.

center with uncertainty $(\delta x_1)_{\rm in}/\sqrt{\nu} = (\delta x_2)_{\rm in}/\sqrt{\nu} = 1/\sqrt{\nu}$; the uncertainties here, distinguished by a δ, are calculated from the Q distribution, i.e., using antinormal ordering. Alternatively, one could amplify the coherent state with an ideal linear amplifier and determine the center of the output state with uncertainty $(\delta x_1)_{\rm out}/\sqrt{\nu} = (\delta x_2)_{\rm out}/\sqrt{\nu} = g/\sqrt{\nu}$; this allows one to determine the center of the input coherent state with the same uncertainty as measurements at the input, i.e., $(\delta x_1)_{\rm out}/g\sqrt{\nu} = (\delta x_2)_{\rm out}/g\sqrt{\nu} = 1/\sqrt{\nu}$. The point of linear amplification is to make a signal much larger so it can be detected by less sensitive measurements. That it is possible to determine the input with exactly the same sensitivity by measuring either the input or the output is an alternative way of characterizing the performance of an ideal amplifier.

It is interesting to apply this sort of thinking to the unphysical amplifiers with $\mu^2 < 1$; if one could construct such an amplifier, one could determine the center of an input coherent state with uncertainty

$$\frac{(\delta x_1)_{\rm out}}{g\sqrt{\nu}} = \frac{(\delta x_2)_{\rm out}}{g\sqrt{\nu}} = \frac{\sqrt{\mu^2(g^2-1)+1}}{g\sqrt{\nu}}. \tag{2.18}$$

This violates the uncertainty-principle bound for any $\mu^2 < 1$ and thus provides another way of seeing why the amplifiers with $\mu^2 < 1$ are unphysical.

A potential way to make such an amplifier physical is to make it nondeterministic, so that it only works with probability $p_{\checkmark}$. Then, since only $p_{\checkmark}\nu$ of the trials are effective, one can determine the center of the input coherent state with uncertainty $(\delta x_1)_{\rm out}/g\sqrt{p_{\checkmark}\nu} = (\delta x_2)_{\rm out}/g\sqrt{p_{\checkmark}\nu}$. Requiring that this uncertainty not best the uncertainty-principle bound,

$$\frac{(\delta x_1)^2_{\rm out}}{p_{\checkmark}g^2} = \frac{(\delta x_2)^2_{\rm out}}{p_{\checkmark}g^2} \geqslant 1, \tag{2.19}$$

gives us a bound on the working probability,

$$p_{\checkmark} \leqslant \frac{(\delta x_1)^2_{\rm out}}{g^2} = \frac{(\delta x_2)^2_{\rm out}}{g^2} = \mu^2 + \frac{1-\mu^2}{g^2}. \tag{2.20}$$

Another way to express the bound (2.20) is in terms of the root-probability–SNR product, $\sqrt{p_{\checkmark}}$SNR, where if x_1 and x_2 represent the amplitude and phase quadratures ($\langle x_1\rangle = \sqrt{2}|\alpha|$ and $\langle x_2\rangle = 0$), the SNR is defined as $\mathrm{SNR} \equiv \langle x_1\rangle/\delta x_1 = \langle x_1\rangle/\delta x_2$. The root-probability–SNR product is a measure of the resolvability of states. The uncertainty-principle bound (2.20) on success probability is equivalent to the requirement that amplification not increase this resolvability, i.e.,

$$\sqrt{p_{\checkmark}}\,\mathrm{SNR}_{\rm out} \leqslant \mathrm{SNR}_{\rm in} = \sqrt{2}|\alpha|. \tag{2.21}$$

The root-probability–SNR product provides the same information as the uncertainty-principle bound, but without referring output quantities to the input. We consider the root-probability–SNR product again in Sec. VI.

It is worth noting that since the output state $\rho_{\rm out}$ is Gaussian, its fidelity with $|g\alpha\rangle$ is the inverse of the antinormally ordered output variances:

$$F(\mu^2) = \langle g\alpha|\rho_{\rm out}|g\alpha\rangle = \pi\, Q_{\rm out}(g\alpha) = \frac{1}{\mu^2(g^2-1)+1}. \tag{2.22}$$

This gives a bound on the probability-fidelity product,

$$p_{\checkmark}(\mu^2)F(\mu^2) \leqslant \frac{1}{g^2}, \tag{2.23}$$

which is independent of μ^2 and achieved by an ideal linear amplifier. The probability-fidelity product can be regarded as the overall probability to reach the target state $|g\alpha\rangle$. Such products appear again throughout our analysis.

For the remainder of the paper, we focus on the immaculate linear amplifier ($\mu^2 = 0$), for which the probability bound (2.20) becomes $p_{\checkmark} \leqslant 1/g^2$. Our analysis shows that a nondeterministic immaculate linear amplifier only works with high fidelity on a portion of phase space, where it has considerably less chance of working than this bound. It thus does considerably worse than a deterministic linear amplifier in determining the center of an input coherent state. This suggests that such devices should not be thought of primarily as linear amplifiers. They could be used, however, as probabilistic, approximate cloners, a task that we consider now.

III. AMPLIFIERS AND CLONING

Exact, deterministic cloning is not allowed by quantum mechanics [4,5,15]. For coherent states, the impossibility of exact, deterministic cloning corresponds to the impossibility of deterministic immaculate amplification. If one has M clones of a coherent state $|\alpha\rangle$, they can be coherently combined in an M-port device to produce $M-1$ vacuum states and a single amplified coherent state $|g\alpha\rangle$, with $g = \sqrt{M}$; running an amplified coherent state $|g\alpha\rangle$ backwards through the same device splits that state into M clones. This equivalence between cloning and immaculate amplification is the basis for links between cloning and amplification (see, e.g., Refs. [4,16]); here we summarize the links and the terminology relevant to this paper [17,18].

The cloning literature phrases the task of cloning in terms of transforming N replicas of the state to be cloned into some number M of identical clones; this is termed "N to M" cloning and is often denoted $N \to M$. An amplifier with amplitude gain g can be thought of as doing $1 \to M = \sqrt{g}$ cloning. Since exact, deterministic cloning is ruled out by the no-cloning theorem when $M > N$, one must drop either exactness, considering instead *noisy* or *approximate* cloning [19], or determinism, considering instead *probabilistic* cloning.

Consider first approximate, deterministic cloning. The standard measure of performance for approximate cloning is the fidelity F of the clones with the desired target state. If the clones all have the same fidelity with the target state, the cloning process is said to be *symmetric*. If the fidelity of the clones is independent of the input state, the cloning is called *universal*.

It is known [17,20] that the optimal fidelity for cloning coherent states $|\alpha\rangle$ to M clones that have Gaussian noise is achieved by using an ideal linear amplifier with gain $g = \sqrt{M}$, followed by an M-port device that splits the amplified state into M approximate clones, each of which has the marginal state ρ_α. The state ρ_α has P function $P_\alpha(\beta) = g^2 P_{\rm out}(g\beta)$ [see Eq. (2.12)], and the corresponding Q distribution is

$$Q_\alpha(\beta) = \frac{e^{-|\beta-\alpha|^2/(2-1/g^2)}}{\pi(2-1/g^2)}. \tag{3.1}$$

The output fidelity,

$$F_{1\to M} = \langle\alpha|\rho_\alpha|\alpha\rangle = \pi\, Q_\alpha(\alpha) = \frac{M}{2M-1}, \tag{3.2}$$

is a function of the gain alone, independent of the amplitude of the input state [17,21]. This output fidelity limits to $\frac{1}{2}$ as $M \to \infty$.

Suppose instead that one desires perfect clones and is thus willing to put aside determinism. This is called exact ($F = 1$), probabilistic cloning [22], and the appropriate measure of performance is the probability $p_\checkmark$ that the cloning process works. In probabilistic cloning, one usually restricts to a finite set of input states and attempts to clone these states optimally. The restriction on input states is referred to as *state-dependent* cloning.

In Sec. V, we consider exact, but probabilistic immaculate amplification. Given the equivalence between immaculate amplification and exact cloning, this can equally well be thought of as exact, probabilistic, $1 \to M = \sqrt{g}$ cloning of coherent states. We show that exact, probabilistic immaculate amplification of all coherent states—or even of all the coherent states on a circle centered at the origin of phase space—cannot occur with a nonzero probability of success. If, however, the input coherent states are restricted to a finite set equally spaced around a circle centered at the origin, exact immaculate amplification can occur with a success probability given by the probability of unambiguously discriminating the input coherent states [9,10]. Once one has identified unambiguously the input state, one can do any state transformation, including making an amplified coherent state or making as many exact clones as one wants. Thus, we have a recipe for making an exact, probabilistic immaculate amplifier or an exact, probabilistic, state-dependent cloner.

In Sec. VI, we derive rigorous bounds on the success probability of an amplifier that amplifies coherent states near the origin immaculately with fidelity near unity, but has output fidelity that decreases to zero as the amplitude of the input coherent states increases. Since the output states do not have Gaussian noise, the connection to cloning is not precise, but for coherent states near the origin, these amplifiers can be thought of as cloners that are approximate, probabilistic, and state dependent.

There is some cloning literature that considers various combinations of approximate, probabilistic, and state-dependent cloning. For example, Chefles and Barnett [23] interpolate between exact, probabilistic, state-dependent cloners and approximate, deterministic cloners, including both fidelity and success probability as performance measures, but only for two input states, a restriction that makes their results too limited for our purposes. There is also work on cloning for a distribution of input coherent states [24], which derives the optimal average fidelity of a $1 \to 2$ cloner that acts on a Gaussian distribution with width Δ centered at the origin. As the width goes to zero, the average fidelity not surprisingly approaches unity.

IV. PRIOR WORK ON PROBABILISTIC IMMACULATE AMPLIFICATION

Ralph and Lund [7] conceived the notion of an immaculate linear amplifier and proposed a probabilistic implementation (what they called a nondeterministic, noiseless linear amplifier) described by a quantum operation

$$\mathcal{E}_{\rm amp}(\rho) = \mathcal{E}_\checkmark(\rho) + \mathcal{E}_{\rm fail}(\rho), \tag{4.1}$$

where $\mathcal{E}_\checkmark$ is the quantum operation when the amplifier works and $\mathcal{E}_{\rm fail}$, the quantum operation when it fails, describes its fallible nature.

Ralph and Lund [7] and collaborators [25] suggested that the most straightforward incarnation of a probabilistic immaculate amplifier is to have

$$\mathcal{E}_\checkmark(|\alpha\rangle\langle\alpha|) = p_\checkmark\, |g\alpha\rangle\langle g\alpha| \tag{4.2}$$

for all input coherent states, where $p_\checkmark$ is the state-independent probability that the amplifier works. Since this makes $\mathcal{E}_\checkmark = p_\checkmark \mathcal{A}$, i.e., a multiple of the map (2.17) for a deterministic immaculate amplifier, it is not completely positive unless the success probability is zero. Indeed, quite generally, if $\mathcal{E}_\checkmark$ works as a linear amplifier with uniform success probability over the entire phase plane, complete positivity imposes the same restrictions on $\mathcal{E}_\checkmark$ as for a deterministic linear amplifier; in particular, $\mathcal{E}_{\rm amp}$ would be just as noisy as a deterministic amplifier, the only difference being that some of the time the amplifier would not work at all. To make an immaculate amplifier physical, one must make it not just probabilistic, but also drop the idea that it can work immaculately over the entire phase plane with uniform success probability. In making models of immaculate amplification, this is precisely what Ralph and Lund [7] and Fiurášek [8] did.

For the remainder of this section, we review some of the theoretical proposals for and experimental realizations of Eq. (4.1). Here implementation is interpreted as meaning that the amplifier works immaculately with high fidelity in a restricted region of phase space near the origin and with the success probability $p_\checkmark$ depending on the distance of the input coherent state from the origin.

Quantum-scissors proposal. Ralph and Lund originally proposed to implement Eq. (4.2) using a network of beam splitters, single-photon sources, and single-photon detectors, as illustrated in Fig. 2. An input coherent state $|\alpha\rangle$ is split up equally at an N-port splitter, each output $|\alpha/\sqrt{N}\rangle$ is processed through a modified "quantum scissors" (MQS) [26], and the outputs of the quantum scissors are recombined at a second N-port splitter. Successful immaculate amplification requires heralding on the MQSs so that they work correctly and on vacuum detection in $N-1$ outputs of the second splitter. These heralding requirements mean that the quantum-scissors proposal is probabilistic, and its region of high-fidelity immaculate amplification is restricted by the requirement that $|\alpha|^2 \ll N$. Even within this phase-plane region, the fidelity with the target state $|g\alpha\rangle$ is a function of the amplitude $|\alpha|$ of the input coherent state.

In Ref. [27], Jeffers tried to reduce the need to make N so large by constructing a quantum-scissors device that works at the two-photon level, i.e., that implements the truncation-and-amplification transformation $|\alpha'\rangle = c_0|0\rangle + c_1|1\rangle + c_2|2\rangle + O(|\alpha'|^3) \to c_0|0\rangle + gc_1|1\rangle + g^2c_2|2\rangle$. Though this is a nice idea, there is a catch: It requires lossy beam splitters or a beamtritter. Numerically it was shown that, for $|\alpha|^2 = 0.1$, a single two-photon device performs better than $N = 3$ single-photon MQSs with respect to the fidelity of the output with

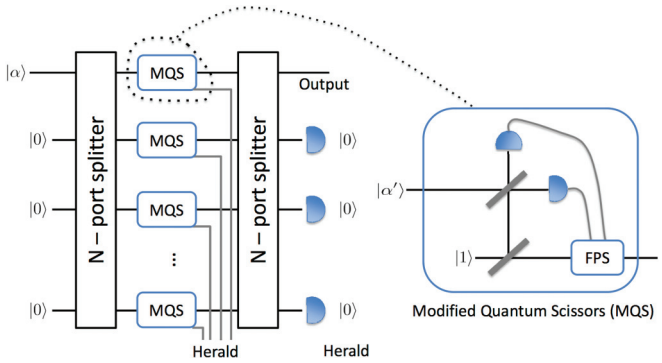

FIG. 2. (Color online) Device that approximates an immaculate amplifier (figure based on Fig. 1 of Ref. [25]). An incident coherent state is split equally into N modes at an N-port splitter. The state of each mode is a coherent state $|\alpha'\rangle$, where $\alpha' = \alpha/\sqrt{N}$; N is chosen large enough that $\alpha' = \alpha/\sqrt{N} \ll 1$, so that $|\alpha'\rangle = |0\rangle + \alpha'|1\rangle + O(|\alpha'|^2)$ is well approximated by its vacuum and one-photon pieces. Each of the N modes enters a modified "quantum scissors" (MQS) [26], shown on the right, which is the heart of the amplifier. When the two detectors in the MQS get results 1,0 or 0,1, the MQS is said to work; a feedforward phase shift (FPS) by π, controlled on one of the two outcomes, is applied to the device's output mode. The result of these manipulations is that, conditioned on the MQS working, it implements the transformation $|\alpha'\rangle \to (1 + g\alpha' a^\dagger)|0\rangle = |g\alpha'\rangle_{\text{trunc}}$, i.e., truncation of the state to the vacuum–one-photon sector and change of the relative weights of the vacuum and one-photon contributions so that the one-photon weight is increased; the gain is determined by the transmissivities and reflectivities of the beam splitters in the MQS. The amplified and truncated states, $|g\alpha'\rangle_{\text{trunc}}$, are recombined at a second N-port splitter. Conditional on detecting vacuum in $N-1$ outputs of this splitter, the output mode is in the amplified state $|g\alpha\rangle$ in the limit that $N \to \infty$. Successful immaculate amplification thus corresponds to heralding on the desired outcome of all of the MQSs, as well as vacuum detection in the $N-1$ ports of the final N-port splitter.

the target amplified state $|g\alpha\rangle$ and the success probability. No mention is made in either Jeffers's or Ralph and Lund's work of how close these implementations are to limits imposed by quantum theory.

Quantum-scissors implementations. One-photon scissors devices have been implemented experimentally by Xiang *et al*. [25] and Ferreyrol *et al*. [28,29].

The experiment by Xiang *et al*. [25] used an attenuated spontaneous parametric down-conversion source to produce an input state $\rho_{\text{in}} = (1 - |\alpha|^2)|0\rangle\langle 0| + |\alpha|^2|1\rangle\langle 1|$, where $|\alpha|^2 \in [10^{-3}, 10^{-1}]$. This state is an approximation to a uniform mixture of coherent states of fixed amplitude; the motivation for considering this input state was to investigate the action of the amplifier on all states in the mixture simultaneously. As the value of $|\alpha|$ was so small, i.e., $\alpha = \alpha'$, only $N = 1$ quantum-scissors device is needed. The domain of gains used in the experiment was $g \in [\sqrt{2}, 2]$. For $g = \sqrt{3}$, the experimental data showed that the amplifier was linear over the range $|\alpha| \in [10^{-3}, 2 \times 10^{-2}]$.

Ferreyrol *et al*. [28,29] implemented quantum-scissors-type amplifiers with $N = 1$, input coherent states with $|\alpha| \in [5.5 \times 10^{-2}, 1]$, and $g \in [0.25, 2]$. Their theoretical modeling and experimental results are in agreement with the modeling and results in Ref. [25]. The first data point is in the region of phase space where the device has linear gain. Very quickly, however, the gain decreases for input states with $|\alpha| > 5.5 \times 10^{-2}$. Their data also show that as the coherent-state amplitude increases, the probability of the amplifier's working increases, and the output state is increasingly distorted away from the target coherent state. These behaviors appear in our analysis of quantum limits on immaculate amplifiers in Sec. VI.

Photon addition and subtraction proposals. Fiurášek [30] and, separately, Marek and Filip [31] attempt to approximate the transformation in Eq. (4.2) by adding and then subtracting M photons from a low-amplitude coherent state. The transformation for $M = 1$ is $aa^\dagger(|0\rangle + \alpha|1\rangle) \to a(|1\rangle + \sqrt{2\alpha}|2\rangle) \to |0\rangle + 2\alpha|1\rangle$, which has a gain of 2. This will not act like a linear amplifier unless $|\alpha| \lesssim 1$. Generalizing to M-photon addition and subtraction, the gain becomes $g = M + 1$. The chief problem with this method is the experimental infeasibility of M-photon addition and subtraction for M more than a very few.

Photon addition and subtraction implementations. Zavatta *et al*. [32] reported an experimental implementation of a single-photon addition and subtraction device ($M = 1$), which had $|\alpha| \in [0.2, 1]$, and $g \in [1.25, 2]$. For input $|\alpha| > 0.5$ the fidelity of the output state with $|g\alpha\rangle$ dropped dramatically, and the appearance of the output Wigner function departed noticeably from the target Wigner function in a way to which we return in Sec. VI. The authors point out that an equivalent quantum-scissors device performs worse with respect to gain and fidelity, both of which decrease quicker with increasing $|\alpha|$ in the scissors case.

Proposals for noise addition followed by photon subtraction. To overcome the difficulties of adding M photons, Marek and Filip [31] suggested one could simply add phase-insensitive noise (random displacements on the phase plane) and then do M-photon subtraction. Intuitively this can be understood as follows: Adding noise increases the phase space area of the state; the subsequent photon subtraction enhances the larger photon numbers, producing an amplified final state that is, roughly speaking, squeezed in the amplitude direction. An explicit formula is given for the success rate as a function of the input coherent state, M, and the mean number of thermal photons added.

Implementation of noise addition followed by photon subtraction. Usuga *et al*. [33] and Usuga [34] describe the preparation of a displaced thermal state which is intended to correspond to a coherent state with added thermal noise. The parameters used in their experiments are $|\alpha| = 0.431$, $g \in [1, 2]$, and $M \in [1, 4]$. For $g > 2$ ($M > 1$), the authors found that the probability of success decreased drastically, and the state started to deform (also see Ref. [35]).

Discussion. From the theory and experiments summarized above, several conclusions can be drawn. First, all of the devices produce an output state with high fidelity to the target coherent state $|g\alpha\rangle$ only over a restricted region of the phase plane centered on the origin. Second, although the theoretical proposals allow for high gains and high input amplitudes, current implementations are restricted to small gains $g \lesssim 2$ and small input amplitudes $|\alpha| \lesssim 2$ by technical limitations. Third, even for these small gains and small input amplitudes, these devices fail almost all of the time.

Most previous work on this subject has focused on proposing and analyzing the performance of specific schemes for probabilistic immaculate amplification. We take a different tack: We provide a general analysis of the performance of any device that attempts to approximate immaculate linear amplification. We characterize the amplifier by its gain and the region of the phase plane over which it operates with high fidelity, and we derive fundamental quantum limits on the probability that the amplifier works.

V. USD BOUNDS ON PROBABILISTIC IMMACULATE AMPLIFICATION

Quantum state discrimination is a decision-theoretic task in which an agent, who has the ability to perform any measurement he wishes, is handed a single state drawn from a known set of states and is told to determine which of the states he received. Our chief interest here is unambiguous state discrimination (USD): The agent is told never to misidentify the state, at the cost of sure and sudden death, but is allowed throw up his hands in despair and refuse to make a decision. A set of states can be discriminated unambiguously if and only if they are linearly independent [9]; there is a nonzero probability for no decision unless the states are orthogonal. In this section we apply USD bounds to the performance of exact immaculate amplifiers. We use the USD formalism in two ways.

The first is to provide upper bounds on the working probability of an immaculate amplifier. Let $\wp(\checkmark)$ be the probability that an immaculate amplifier works exactly on a set of input coherent states. Suppose that P^{B} is the optimal probability for discriminating the input states and P^{A} is the corresponding optimal probability for discriminating the amplified states. The amplified states, being further apart on the phase plane than the input states, are easier to distinguish, so $P^{\mathrm{A}} > P^{\mathrm{B}}$. The overall probability of successfully discriminating the amplified states is $\wp(\checkmark)P^{\mathrm{A}}$. Since P^{B} is optimal, the amplification process cannot increase the distinguishability of the states, so we must have $P^{\mathrm{B}} \geqslant \wp(\checkmark)P^{\mathrm{A}}$. The result is a strict upper bound, $\wp(\checkmark) \leqslant P^{\mathrm{B}}/P^{\mathrm{A}}$, on the probability that the immaculate amplifier works; we cannot warrant, however, that this upper bound can be achieved.

The second way we use the USD formalism is to construct models of immaculate amplifiers that have an achievable working probability. Once one has used USD to identify one of the input states, one can perform any unitary transformation on that state. This procedure always produces the right transformed state when it makes a decision; consequently, we call it, somewhat cumbersomely, an *exact, finite-state, probabilistic state transformation*. The transformation could be the displacement of a coherent state required to amplify it. Since the optimal USD discrimination probability P^{B} can be achieved in principle, the result is a model for an immaculate amplifier that works with probability P^{B} on a finite set of input coherent states. We call such a model a *finite-state, probabilistic immaculate amplifier*.

We note this formulation and subsequent analysis is similar to the analysis performed by Dunjko and Andersson in Ref. [36]. Their results are not explicit about the dependence of the success probabilities on gain and input amplitude, whereas we are.

A. Helstrom bound for two coherent states

Before turning to USD bounds on immaculate amplifiers, we consider a related bound provided by the minimal error probability in discriminating two nonorthogonal states. Consider two coherent states, $|\alpha\rangle$ and $|\beta\rangle$. A measurement that minimizes the chance of incorrectly identifying the state is known as a Helstrom discrimination measurement [37,38]. The probability of successful identification is

$$P^{\mathrm{B}}_{\mathrm{Hel}}(\checkmark) = \tfrac{1}{2}(1+\sqrt{1-|\langle\beta|\alpha\rangle|^2}) = \tfrac{1}{2}(1+\sqrt{1-e^{-|\alpha-\beta|^2}}), \tag{5.1}$$

where the superscript "B" reminds us that this probability is *before* immaculate amplification. It is apparent that as the separation, $|\alpha-\beta|$, between the two states grows, the states become orthogonal, and the probability of successful discrimination approaches unity. In contrast, when $|\alpha-\beta| \to 0$, the success probability limits to guessing.

Now we use the above-described procedure, modified to Helstrom discrimination, to bound the working probability $\wp(\checkmark)$ of an immaculate amplification device. The device takes $|\alpha\rangle$ to $|g\alpha\rangle$ and $|\beta\rangle$ to $|g\beta\rangle$. Amplification increases the distinguishability of the states so that the probability of successful identification of the state is

$$P^{\mathrm{A}}(\checkmark) = \tfrac{1}{2}(1+\sqrt{1-e^{-g^2|\alpha-\beta|^2}}), \tag{5.2}$$

where the superscript "A" reminds us this is *after* amplification. The overall probability to identify the input state correctly after amplification is

$$P^{\mathrm{A}}_{\mathrm{Hel}}(\checkmark) = \tfrac{1}{2}[1-\wp(\checkmark)] + \wp(\checkmark)P^{\mathrm{A}}(\checkmark) = \tfrac{1}{2}[1+\wp(\checkmark)\sqrt{1-e^{-g^2|\alpha-\beta|^2}}]. \tag{5.3}$$

Since the probability for successful discrimination cannot increase, we must have $P^{\mathrm{A}}_{\mathrm{Hel}}(\checkmark) \leqslant P^{\mathrm{B}}_{\mathrm{Hel}}(\checkmark)$, which gives an upper bound on the amplifier's success probability,

$$\wp(\checkmark) \leqslant \sqrt{\frac{1-e^{-|\alpha-\beta|^2}}{1-e^{-g^2|\alpha-\beta|^2}}}. \tag{5.4}$$

This bound, which holds for any pair of states, has its minimum value when the two coherent states become very close to each other, i.e., $|\alpha-\beta| \to 0$; in this case the bound on the working probability becomes

$$\wp_{\mathrm{Hel}} \leqslant \frac{1}{g}. \tag{5.5}$$

For constructing models of immaculate amplifiers, Helstrom-type discrimination has the problem that it sometimes misidentifies the input state. Such misidentification inevitably leads to noise in the amplifier output, which cannot be part of a model of an exact immaculate amplifier.

B. USD bounds

1. Two coherent states

Unambiguous state discrimination does discriminate states without error, but this providence requires a sacrifice, namely, the no-decision measurement result. For two input states, $|\alpha\rangle$

and $|\beta\rangle$, the probability of successfully identifying them is [38]

$$P^{\mathrm{B}}_{\mathrm{USD}}(\checkmark) = 1 - |\langle\beta|\alpha\rangle|^2 = 1 - e^{-|\alpha-\beta|^2}. \tag{5.6}$$

In this expression, as in the Helstrom case, it is apparent that as the separation, $|\alpha - \beta|$, between the two states grows, the probability of discrimination approaches unity. When the states get close together, $|\alpha - \beta| \to 0$, the probability of successful discrimination goes to zero.

After amplification we have a discrimination probability,

$$P^{\mathrm{A}}(\checkmark) = 1 - |\langle g\beta|g\alpha\rangle|^2 = 1 - e^{-g^2|\alpha-\beta|^2} \tag{5.7}$$

and an overall probability for successfully identifying the input state,

$$P^{\mathrm{A}}_{\mathrm{USD}}(\checkmark) = \wp(\checkmark)\, P^{\mathrm{A}}(\checkmark). \tag{5.8}$$

Since amplification cannot increase the distinguishability of the states, we have $P^{\mathrm{A}}_{\mathrm{USD}}(\checkmark) \leqslant P^{\mathrm{B}}_{\mathrm{USD}}(\checkmark)$ and thus an upper bound on the working probability,

$$\wp(\checkmark) \leqslant \frac{P^{B}_{\mathrm{USD}}(\checkmark)}{P^{A}(\checkmark)} = \frac{1 - e^{-|\alpha-\beta|^2}}{1 - e^{-g^2|\alpha-\beta|^2}}, \tag{5.9}$$

as pointed out in Ref. [25]. Being the square of the Helstrom bound (5.4), this is always the tighter bound. The minimum of the bound is found in the limit that the coherent states become very close to each other, i.e., $|\alpha - \beta| \to 0$, in which case the bound becomes

$$\wp_{\mathrm{USD}} \leqslant \frac{1}{g^2}. \tag{5.10}$$

The allowed working probability is a factor of $1/g$ smaller than the Helstrom bound (5.5). This USD bound is the same as the bound (2.20), which was derived by considering how to distinguish neighboring coherent states using quadrature measurements; the two bounds are the same because both are based on discriminating neighboring coherent states.

2. *M coherent states on a circle*

The USD bound (5.10) is not at all a tight bound on the working probability for a probabilistic immaculate amplifier. We can get much tighter bounds by applying USD to more than two input states. Indeed, we work toward a phase-insensitive amplifier, which must act symmetrically on *all* input coherent states with the same $|\alpha|$. Thus, what we do is to consider a set of M coherent states, $|\alpha_j\rangle = |\bar{\alpha}e^{i\phi_j}\rangle$, all located on a circle of radius $\bar{\alpha}$ with phases

$$\phi_j = \frac{2\pi j}{M}, \quad j = 0,1,2,\ldots,M-1, \tag{5.11}$$

distributed uniformly around the circle. To avoid clutter in what follows, we use, as here, $\bar{\alpha} = |\alpha|$. To apply USD to the states $|\alpha_j\rangle$, they must be linearly independent. This property was shown in Ref. [39], and it emerges naturally as part of the USD construction. In contrast, the continuum of states on the circle are complete, spanning the entire Hilbert space, but are not linearly independent; we review these facts in Appendix A.

Chefles and Barnett [10] solved the USD problem for sets of linearly independent symmetric states (see also [9]). For the case of coherent states on a circle, the unitary operator that rotates between states is the phase-plane rotation by angle $2\pi/M$, i.e., $U = e^{i2\pi a^\dagger a/M}$. Restricted to the subspace spanned by the set of input coherent states, U has the eigendecomposition

$$U = \sum_{r=0}^{M-1} e^{i\phi_r}\, |\gamma_r\rangle\, \langle\gamma_r|\,, \tag{5.12}$$

where the (orthonormal) eigenstates are given by

$$c_r\, |\gamma_r\rangle = \frac{1}{M} \sum_{j=0}^{M-1} e^{-i2\pi rj/M} |\alpha_j\rangle. \tag{5.13}$$

Here c_r, chosen to be real, is the magnitude of the vector on the right:

$$\begin{aligned} c_r^2 &= \frac{1}{M} \sum_{j=0}^{M-1} e^{-i2\pi rj/M} \langle\alpha_0|\alpha_j\rangle \\ &= \frac{1}{M} \sum_{j=0}^{M-1} e^{-ir\phi_j} \exp[\bar{\alpha}^2(e^{i\phi_j} - 1)]. \end{aligned} \tag{5.14}$$

It is useful to manipulate c_r^2 into a quite different form and also to write it in terms of

$$\begin{aligned} q_r = Mc_r^2 &= e^{-\bar{\alpha}^2} \frac{d^{M-r}}{dx^{M-r}} \sum_{j=0}^{M-1} \exp(xe^{i\phi_j})\Big|_{x=\bar{\alpha}^2} \\ &= Me^{-\bar{\alpha}^2} \sum_{k=0}^{\infty} \frac{\bar{\alpha}^{2(kM+r)}}{(kM+r)!}. \end{aligned} \tag{5.15}$$

That the states $|\gamma_r\rangle$ are orthonormal establishes that they and the original coherent states $|\alpha_j\rangle$ span an M-dimensional subspace and thus that the $|\alpha_j\rangle$ are linearly independent.

The vectors

$$|\alpha_j^{\perp}\rangle = \frac{1}{M} \sum_{r=0}^{M-1} \frac{1}{c_r} e^{i2\pi rj/M}\, |\gamma_r\rangle \tag{5.16}$$

are reciprocal (or dual) to the original coherent states in the sense that $\langle\alpha_j^{\perp}|\alpha_k\rangle = \delta_{jk}$. This duality property is what is needed to construct the USD positive-operator-valued measure (POVM). This POVM has M POVM elements $E_j = P(\checkmark)|\alpha_j^{\perp}\rangle\langle\alpha_j^{\perp}|$, $j = 0,\ldots,M-1$, for the results that identify the input states, where $P(\checkmark)$ is the success probability, and a single failure POVM element, $E_{\mathrm{fail}} = I - E$, where

$$E = \sum_j E_j = P(\checkmark) \sum_r \frac{1}{q_r}\, |\gamma_r\rangle\, \langle\gamma_r|\,. \tag{5.17}$$

The largest eigenvalue of E must be no larger than 1, which gives an optimal success probability for discriminating among M coherent states symmetrically placed on a circle of radius $\bar{\alpha}$ [10]:

$$P(\checkmark|\bar{\alpha}, M) = \min_{r\,\in\,\{0,\ldots,M-1\}} q_r. \tag{5.18}$$

This success probability has two important limits: (i) many states on the circle or, equivalently, small coherent-state amplitude, i.e., $M \gg \bar{\alpha}^2$, and (ii) states sparse on the circle or, equivalently, large coherent-state amplitude, i.e., $M \ll \bar{\alpha}$.

The reason for the difference in powers of $\bar{\alpha}$ in the two limits emerges as we examine each limit in turn.

Notice first that the sums for q_r/M in Eq. (5.15) consist of terms drawn with period M from a Poisson distribution that has mean $\bar{\alpha}^2$, a distribution we denote throughout by $\Pr[\,n|\bar{\alpha}^2\,] = e^{-\bar{\alpha}^2}\bar{\alpha}^{2n}/n!$. When the first term in the sum for $r = M-1$ lies beyond the maximum of the Poisson distribution, as it does in the case of many states on the circle, it takes only a moment's contemplation to realize that the terms in the sum for q_{M-1} are term by term smaller than the corresponding terms in the sums for other values of r, provided that the first term in q_{M-1} is smaller than the first term in q_0, i.e., $\bar{\alpha}^{2(M-1)}/(M-1)! < 1$, which is certainly true when $M \gg \bar{\alpha}^2$. Thus, for many coherent states on the circle, the minimum in Eq. (5.18) is achieved by $r = M-1$ [10], so

$$P(\checkmark|\bar{\alpha},M) = q_{M-1} = Me^{-\bar{\alpha}^2}\sum_{k=0}^{\infty}\frac{\bar{\alpha}^{2(kM+M-1)}}{(kM+M-1)!}. \quad (5.19)$$

Moreover, the Chernoff bound for a Poisson random variable n with mean $\bar{\alpha}^2$ [40], applied to the terms in the sum (5.19) after the first,

$$\sum_{k=1}^{\infty}\frac{\bar{\alpha}^{2(kM+M-1)}}{(kM+M-1)!} < e^{\bar{\alpha}^2}\Pr[\,n \geqslant 2M-1|\bar{\alpha}^2\,] \leqslant \left(\frac{e\bar{\alpha}^2}{2M-1}\right)^{2M-1}, \quad (5.20)$$

shows that, in the limit $M \gg \bar{\alpha}^2$, we need to keep only the first term, $k = 0$, of the sum (5.19). The result is a simple expression for USD success probability in the case of many coherent states on a circle (small coherent-state amplitude):

$$P(\checkmark|\bar{\alpha},M) = \frac{Me^{-\bar{\alpha}^2}\bar{\alpha}^{2(M-1)}}{(M-1)!}, \quad M \gg \bar{\alpha}^2. \quad (5.21)$$

Now consider the case of sparse coherent states on the circle. For fixed M, as $\bar{\alpha} \to \infty$, Chefles and Barnett [10] showed that all of the q_r limit to 1, so

$$P(\checkmark|\bar{\alpha},M) = 1. \quad (5.22)$$

Since, for fixed M, the input states limit to being orthogonal as $\bar{\alpha} \to \infty$, this simply means that orthogonal states can be discriminated with unity probability of success. More useful than the limit, however, is the correction to the limit.

To find this correction, we begin by noting that since $\bar{\alpha} \gg M \geqslant 2$, we can approximate the Poisson distribution in Eq. (5.15) as a Gaussian of the same mean and variance and extend the sum on k to $-\infty$ on the grounds that the Gaussian is negligible for these additional terms:

$$q_r = \frac{M}{\sqrt{2\pi}\bar{\alpha}}\sum_{k=-\infty}^{\infty}\exp\left(-\frac{(kM+r-\bar{\alpha}^2)^2}{2\bar{\alpha}^2}\right). \quad (5.23)$$

By introducing δ functions, we can write this in the form

$$q_r = \frac{M}{\sqrt{2\pi}\bar{\alpha}}\sum_{k=-\infty}^{\infty}\int_{-\infty}^{\infty}dx\,e^{-(x-\bar{\alpha}^2)^2/2\bar{\alpha}^2}\delta(x-kM-r) = \frac{1}{\sqrt{2\pi}}\int_{-\infty}^{\infty}du\,e^{-u^2/2}\sum_{k=-\infty}^{\infty}\delta\left(k-\frac{\bar{\alpha}}{m}+\frac{s-u}{m}\right), \quad (5.24)$$

where x is a continuous version of $kM+r$ and where in the second expression we introduce the integration variable $u = x/\bar{\alpha} - \bar{\alpha}$ and rescaled variables $m = M/\bar{\alpha} \ll 1$ and $s = r/\bar{\alpha} \ll 1$. Now we write $\bar{\alpha}/m = [\bar{\alpha}/m] + \aleph$, where $[z]$ denotes the nearest integer to z and, hence, $-\frac{1}{2} \leqslant \aleph < \frac{1}{2}$ (half-integers are rounded up), redefine the dummy summing variable to be $k - [\bar{\alpha}/m]$, and use

$$\sum_{k=-\infty}^{\infty}\delta(k-v) = \sum_{j=-\infty}^{\infty}e^{-i2\pi jv} \quad (5.25)$$

to put Eq. (5.24) in the form

$$q_r = \frac{1}{\sqrt{2\pi}}\sum_{j=-\infty}^{\infty}e^{i2\pi j(s/m-\aleph)}\int_{-\infty}^{\infty}du\,e^{-u^2/2}e^{-i2\pi ju/m} = 1+2\sum_{j=1}^{\infty}\cos\left[2\pi j\left(\frac{s}{m}-\aleph\right)\right]e^{-2\pi^2j^2/m^2} = \theta_3\left[\pi\left(\frac{s}{m}-\aleph\right);e^{-2\pi^2/m^2}\right]. \quad (5.26)$$

Here θ_3 denotes a Jacobi θ function [41].

When $m \ll 1$, we only need to keep the $j = 1$ term in the sum to get the dominant correction to unity in q_r. To minimize q_r, we choose $r/M - \aleph = s/m - \aleph$ as close to $\frac{1}{2}$ as possible, consistent with letting r be an integer. Thus, we choose $r = [M(\aleph + \frac{1}{2})]$, which gives

$$\cos\left[2\pi\left(\frac{s}{m}-\aleph\right)\right] = -1+\left(\text{irrelevant errors of size } \lesssim \frac{\pi^2}{2M^2}\right). \quad (5.27)$$

Keeping more terms in the sum and then minimizing could provide a better approximation, but the lowest-order, $j = 1$ correction already provides a good approximation for a reasonably dense set of coherent states so the following analysis is restricted to it.

The resulting success probability in the case of sparse coherent states (large coherent-state amplitudes) is

$$P(\checkmark|\bar{\alpha},M) = 1-\epsilon \simeq 1-2e^{-2\pi^2\bar{\alpha}^2/M^2}, \quad M \ll \bar{\alpha}. \quad (5.28)$$

The key result here is that in this limit the success probability only depends on the ratio $\bar{\alpha}/M$. Indeed, using this expression, we can turn the question around and determine the ratio that gives a deviation ϵ:

$$\frac{\bar{\alpha}^2}{M^2} \equiv a(\epsilon) \simeq -\frac{\ln(\epsilon/2)}{2\pi^2} = -0.050\,66\ln\epsilon + 0.0351. \quad (5.29)$$

For example, to achieve $P(\checkmark|\bar{\alpha},M) = 0.9$ for any M, one chooses $\bar{\alpha}^2 \simeq 0.15M^2$. The dependence (5.29) has been tested numerically over the ranges $\epsilon \in [0.5, 10^{-5}]$ and $M \in [2,40]$; the numerics give

$$a(\epsilon) = -0.0508\ln\epsilon + 0.035, \quad (5.30)$$

in good agreement with the analytic approximation. Figure 3 compares the numerics with the analytic approximation; the analytic approximation works quite well for $\epsilon \leqslant 0.5$.

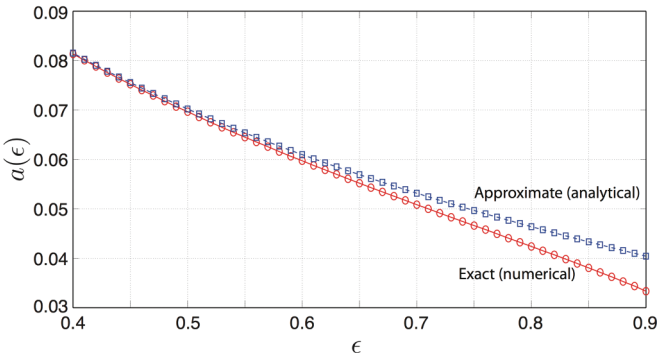

FIG. 3. (Color online) Dependence of the ratio $\bar{\alpha}^2/M^2 = a(\epsilon)$ on the deviation ϵ of the success probability $P(\checkmark|\bar{\alpha},M)$ from unity: Numerical results are plotted as (red) circles; analytic approximation of Eq. (5.29) as (blue) squares. The analytic approximation works quite well for $\epsilon \in [0,0.5]$, but breaks down progressively beyond $\epsilon = 0.5$.

Figure 4 plots the success probability for USD of coherent states on a circle, comparing the exact, numerically determined result with the approximations that apply for many coherent states and sparse coherent states. The two approximations work better than we have any right to expect: The plots and a consideration of the next term in the sum (5.19) suggest that the many-coherent-states approximation (5.21) works well for $M \gtrsim 2\bar{\alpha}^2$; provided $\bar{\alpha}$ is somewhat bigger than 1, the sparse-coherent-states approximation (5.28) works well for $M \lesssim 4\bar{\alpha}$. The two approximations overlap when $\bar{\alpha} \gtrsim 1$ and M are both small, but because of the different powers of $\bar{\alpha}$ in the two approximations, generally there is a gap between the two that must be filled in with numerics.

These results in hand, we can apply them, first, to obtain bounds on the success probability of immaculate amplifiers and, second, to constructing a model of an immaculate amplifier based on USD. For the first task, we use the same notation as previously for before and after probabilities of USD; the USD bound on the success probability of an immaculate amplifier that works on the M input coherent states is

$$\wp(\checkmark|\bar{\alpha},M) \leqslant \frac{P^B_{\rm USD}(\checkmark)}{P^A(\checkmark)} = \frac{P(\checkmark|\bar{\alpha},M)}{P(\checkmark|g\bar{\alpha},M)}. \qquad (5.31)$$

The important cases of this bound require only our approximate results for the USD success probabilities.

A first such case is when the input coherent states are sparse and, hence, so are the amplified output states. In this case, the numerator and the denominator in the bound (5.31) are both close to one, and the bound on success probability is also close to one, reflecting the fact that one can discriminate and amplify such nearly orthogonal states.

More interesting is the case of many input coherent states, $M \gg \bar{\alpha}^2$. If the gain is large enough that the amplified states are sparse, i.e., $M \ll g\bar{\alpha}$—this requires that $g \gg \bar{\alpha}$—the bound (5.31) reduces to

$$\wp(\checkmark|\bar{\alpha},M) \leqslant P^B_{\rm USD}(\checkmark) = \frac{Me^{-\bar{\alpha}^2}\bar{\alpha}^{2(M-1)}}{(M-1)!}. \qquad (5.32)$$

This bound, which is plotted in Fig. 4 as (red) circles in the left column and a (red) dashed line in the right column, can

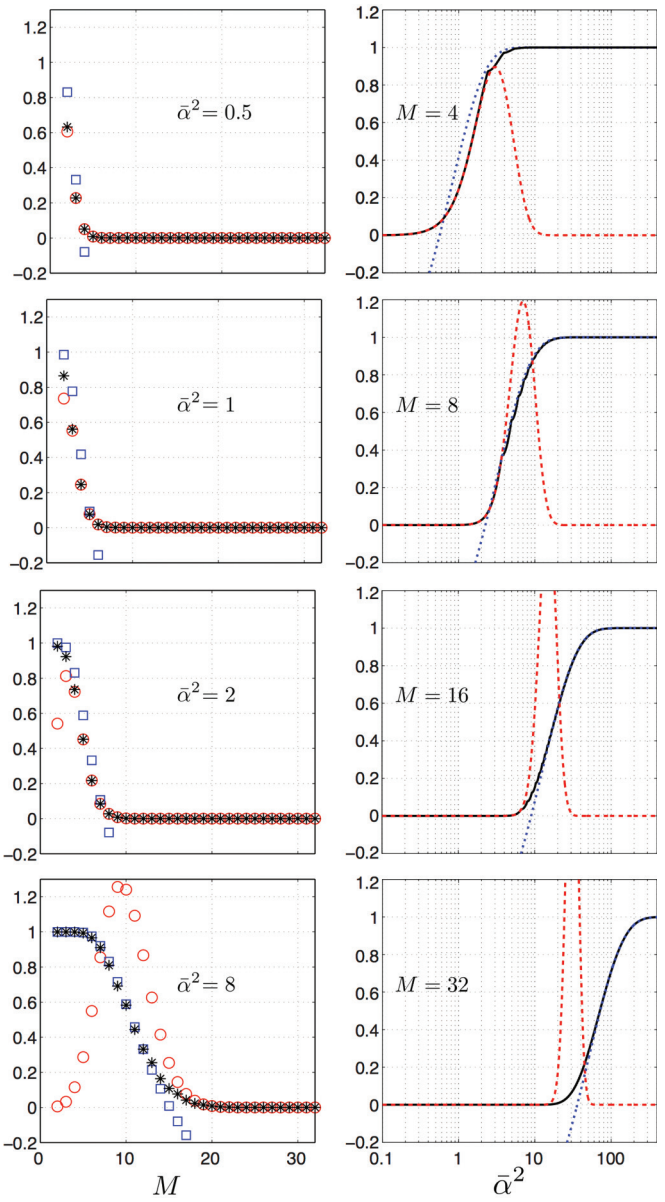

FIG. 4. (Color online) Success probability $P(\checkmark|\bar{\alpha},M) = P^{\rm B}(\checkmark)$. (Left column) As a function of M with fixed $\bar{\alpha}^2$; (black) asterisks are the exact, numerically determined success probability (5.18); (red) circles give the approximate result (5.21) for many coherent states (small coherent-state amplitude); (blue) squares give the approximate result (5.28) for sparse coherent states (large coherent-state amplitude). (Right column) As a function of $\bar{\alpha}^2$ with fixed M; (black) solid line is the exact result; (red) dashed line, many coherent states; (blue) dotted line, sparse coherent states.

be regarded as the $g \to \infty$ bound on an immaculate amplifier that works on a fixed number $M \gg \bar{\alpha}^2$ of input states.

Most interesting is the case in which M is large enough that both the input and amplified output can be treated in the many-coherent-states limit, i.e., $M \gg g^2\bar{\alpha}^2$. In this case, the bound (5.31) becomes $\wp(\checkmark|\bar{\alpha},M) \leqslant e^{(g^2-1)\bar{\alpha}^2}/g^{2(M-1)}$. This case is the most interesting because we can let M become arbitrarily large and thus approach the limit in which the amplifier acts phase-insensitively on the entire circle of coherent states. Since

$M-1 \gg (g^2-1)\bar{\alpha}^2$, we have $e^{(g^2-1)\bar{\alpha}^2} \ll e^{M-1}$ and thus

$$\wp(\checkmark|\bar{\alpha},M) \leqslant \frac{e^{(g^2-1)\bar{\alpha}^2}}{g^{2(M-1)}} \ll \left(\frac{\sqrt{e}}{g^2}\right)^{2(M-1)}. \quad (5.33)$$

This shows that the success probability of an exact immaculate amplifier goes to zero in the phase-insensitive limit $M \to \infty$, even when the amplifier is only required to work on a single circle of input coherent states.

We can make a more precise statement for an immaculate amplifier that amplifies exactly all the coherent states on M spokes spaced equally in angle and of length $\bar{\alpha}$. Such an amplifier acts immaculately on M coherent states on all circles with radius $\leqslant\bar{\alpha}$. The success probability is bounded by the $\bar{\alpha} \to 0$ limit of the bound (5.33), where the assumptions underlying the bound are satisfied for any $M \geqslant 2$:

$$\wp_{\mathrm{USD}} \leqslant \frac{1}{g^{2(M-1)}}. \quad (5.34)$$

This is one of the two chief results of this section: an immaculate amplifier that works exactly on M spokes within a phase-space disk centered at the origin has a working probability that decreases exponentially with M, with the base of the exponential, g^2, given by the gain, and goes to zero in the phase-insensitive limit $M \to \infty$.

It is useful to pause here to relate these results to the discussion at the end of Sec. II. For the disk amplifier, the measurement-based performance measure (2.19), which uses antinormal ordering to calculate the uncertainties, is $1/\wp_{\mathrm{USD}}g^2 \geqslant g^{2(M-2)}$; this is greater than the uncertainty-principle lower bound of one, achieved by an ideal linear amplifier, for $M > 2$ and far worse than the bound as M gets large. (These same arguments hold for the bound on the root-probability–SNR product, which is equivalent to the uncertainty bound.) The related probability-fidelity product is given by $\wp_{\mathrm{USD}} \leqslant 1/g^{2(M-1)}$, since an exact immaculate amplifier has unit output fidelity; this is worse than the probability-fidelity product $1/g^2$ achieved by an ideal linear amplifier for $M \geqslant 2$ and far worse as M gets large.

As we discussed in the introductory paragraphs of this section, we can construct a USD-based model of an immaculate amplifier in which the M input coherent states are first discriminated and then the identified input is amplified immaculately by any amount. The quantum operation for this model is

$$\mathfrak{A}(\rho) = \sum_{j=0}^{M-1} \wp(\checkmark|\bar{\alpha},M)|g\alpha_j\rangle\langle\alpha_j^{\perp}|\rho|\alpha_j^{\perp}\rangle\langle g\alpha_j|. \quad (5.35)$$

This map can be applied to any input state, not just the M coherent states used to construct it, but applied to one of those special input states, $|\alpha_j\rangle$, $\mathfrak{A}$ outputs the amplified state $|g\alpha_j\rangle$ with probability

$$\wp(\checkmark|\bar{\alpha},M) = P^B_{\mathrm{USD}}(\checkmark) = P(\checkmark|\bar{\alpha},M). \quad (5.36)$$

This success probability is plotted in Fig. 4.

When $M \gg \bar{\alpha}^2$, the success probability is given by Eq. (5.21),

$$\wp(\checkmark|\bar{\alpha},M) \simeq \sqrt{\frac{M}{2\pi}}e^{-\bar{\alpha}^2}\left(\frac{e\bar{\alpha}^2}{M-1}\right)^{M-1}, \quad (5.37)$$

where here we apply Stirling's approximation to the factorial to make clear that the success probability goes to zero in the phase-insensitive limit $M \to \infty$.

The case of sparse input states is where immaculate amplification shines with the radiance its name evokes. As the plots in Fig. 4 show, the success probability for this case is captured by the sparse-states approximation (5.28), which is plotted in Fig. 4 as (blue) squares in the left column and a (blue) dotted line in the right column. The approximation works well for success probabilities $1-\epsilon \gtrsim 0.5$, which corresponds to $M \lesssim 4\bar{\alpha}$. To achieve a success probability $1-\epsilon$ requires that $\bar{\alpha}/M = \sqrt{a(\epsilon)}$ be chosen as in Eq. (5.29). To get a feeling for what these results mean, notice that a success probability of $1-\epsilon$ corresponds to a distance between states, measured along the arc of the circle, given by $2\pi\bar{\alpha}/M = 2\pi\sqrt{a(\epsilon)}$; for example, a success probability of 0.5 corresponds to $\sqrt{a} \simeq 0.265$ and a distance of about 1.67. These states might seem pretty crowded, but the distance makes sense when compared with the one-standard-deviation diameter of a coherent state, which is 1. These input states are just beginning to overlap, but they are far enough apart that they can be distinguished and amplified immaculately half the time.

The lesson here is important: USD-based devices can outperform ideal linear amplifiers if they are both phase-sensitive and amplitude-specific, amplifying immaculately only a relatively sparse set of input coherent states on a particular input circle. This realization leads to a set of interesting questions that we consider briefly in the Conclusion as the basis for future work. The flip side is that success probability goes to zero when an exact immaculate device is required to work phase-insensitively on even a single input circle. This suggests that phase insensitivity is a key property, which does not play well with exact immaculate amplification. In the next section, we explore this further by considering probabilistic immaculate amplifiers that are required to be phase insensitive but, unlike USD-based amplifiers, are not exact.

VI. BOUNDS ON PHASE-INSENSITIVE, APPROXIMATE, PROBABILISTIC IMMACULATE AMPLIFICATION

In this section we canonize phase insensitivity as a primary requirement for amplification. This means that the amplifier's operation must be invariant under phase-plane rotations. We relax the requirement of unit fidelity with the target output state, thus obtaining a model of an approximate immaculate amplifier. We would like the amplifier to work with high fidelity for input coherent states $|\alpha\rangle$ within a disk centered at the origin, but we allow the fidelity with the target amplified state $|g\alpha\rangle$ to fall off for inputs outside the disk of interest. There are two motivations for this assumption: First, as we noted in Sec. IV, an immaculate amplifier cannot work over the entire phase plane; second, as was true for the implementations reviewed in Sec. IV, such a cutoff is a property of practical devices.

We characterize the high-fidelity output region as a disk of radius $\sqrt{N}$; the corresponding input disk thus has radius $\sqrt{N}/g$. After translating this description into the language of amplifier maps and Kraus operators, we characterize the amplifier in terms of the fidelity with the target state, $F(\bar{\alpha})$,

and the probability that the amplifier works, $p(\checkmark|\bar{\alpha})$, both of which are functions of the input amplitude $\bar{\alpha} = |\alpha|$. We maximize the fidelity at each $\bar{\alpha}$ given a working probability at that $\bar{\alpha}$, after which we maximize the working probability consistent with the amplifier's map being trace decreasing. We thus obtain an optimal immaculate amplifier that is both approximate and probabilistic.

We note that a similar analysis has been performed by Fiurášek [8,42] in the context of cloning and arbitrary state transformations; we point out below similarities to and differences from our analysis.

We describe the amplification process by a quantum operation, which we write in terms of a canonical Kraus decomposition in which the Kraus operators are orthogonal. We assume that these Kraus operators have the form $P_N K_j$, where P_N is the projector onto the subspace S_N spanned by the first $N+1$ number states. The amplifier quantum operation is thus

$$\mathcal{A}_N = \sum_j P_N K_j \odot K_j^\dagger P_N, \tag{6.1}$$

where the $\odot$, technically a tensor product, can be regarded as designating the slot for the input to the quantum operation. The projector P_N provides a sharp cutoff in the number basis, beyond which the amplifier's output has no support; notice that we can let the operators K_j map outside S_N without having any effect on the quantum operation (6.1). Shortly we extend the Kraus operators in a way that allows the outputs to have support outside S_N; this extension smooths the rough edges in the amplifier map (6.1), and it provides marginal improvements in the output fidelity. Phase insensitivity is the requirement that $\mathcal{A}_N$ commutes with phase-plane rotations; this implies, as we show in Appendix B, that each Kraus operator has nonzero number-basis matrix elements on only one diagonal strip, as in Eq. (B5). Additionally, the Kraus operators must satisfy the trace-decreasing requirement,

$$\sum_j K_j^\dagger P_N K_j \leqslant I. \tag{6.2}$$

Suppose now that the input state to the amplifier is a coherent state $|\alpha\rangle$. The probability of outcome j is

$$p_j(\checkmark|\bar{\alpha}) = \langle\alpha|K_j^\dagger P_N K_j|\alpha\rangle, \tag{6.3}$$

and the overall success probability is

$$p(\checkmark|\bar{\alpha}) = \sum_j p_j(\checkmark|\bar{\alpha}) = \mathrm{tr}[\mathcal{A}_N(|\alpha\rangle\langle\alpha|)]. \tag{6.4}$$

The fidelity of the output with the target output state $|g\alpha\rangle$ is

$$F(\bar{\alpha}) = \frac{\langle g\alpha|\mathcal{A}_N(|\alpha\rangle\langle\alpha|)|g\alpha\rangle}{p(\checkmark|\alpha)}. \tag{6.5}$$

Because of the rotational symmetry, these quantities depend only on the magnitude $\bar{\alpha} = |\alpha|$.

The problem we solve is the following. Fix a circle of coherent states with amplitude $\bar{\alpha}$, and find the maximum fidelity $F(\bar{\alpha})$ on this circle for a fixed success probability $q = p(\checkmark|\bar{\alpha})$. We do this first for a single Kraus operator and later argue that a single Kraus operator is better than more than one. The optimization problem is thus to maximize

$$F(\bar{\alpha}) = \frac{|\langle g\alpha|P_N K|\alpha\rangle|^2}{p(\checkmark|\bar{\alpha})}, \tag{6.6}$$

subject to the constraint

$$q = p(\checkmark|\bar{\alpha}) = \langle\alpha|K^\dagger P_N K|\alpha\rangle. \tag{6.7}$$

We can, of course, rephrase this as maximizing $|\langle g\alpha|P_N K|\alpha\rangle|^2$ subject to the constraint on working probability.

Introducing a Lagrange multiplier μ, we maximize

$$|\langle g\alpha|P_N K|\alpha\rangle|^2 - \mu(\langle\alpha|K^\dagger P_N K|\alpha\rangle - q). \tag{6.8}$$

Varying K gives

$$\begin{aligned} 0 = {} & \langle\alpha|\delta K^\dagger (P_N|g\alpha\rangle\langle g\alpha|P_N K|\alpha\rangle - \mu P_N K|\alpha\rangle) \\ & + (\text{Hermitian conjugate}), \end{aligned} \tag{6.9}$$

so we conclude that

$$P_N K|\alpha\rangle = P_N|g\alpha\rangle\frac{\langle g\alpha|P_N K|\alpha\rangle}{\mu}. \tag{6.10}$$

The Lagrange multiplier is given by the probability for the first $N+1$ photons in the target state $|g\alpha\rangle$,

$$\mu = \langle g\alpha|\, P_N\, |g\alpha\rangle = e^{-g^2|\alpha|^2} e_N(g^2|\alpha|^2), \tag{6.11}$$

where we introduce a standard shorthand for the first $N+1$ terms in the expansion of the exponential,

$$e_N(x) \equiv \sum_{n=0}^{N} \frac{x^n}{n!}. \tag{6.12}$$

Without changing the Kraus operator $P_N K$, we can let K map outside the subspace S_N in such a way that

$$K|\alpha\rangle = |g\alpha\rangle\frac{\langle g\alpha|P_N K|\alpha\rangle}{\mu}. \tag{6.13}$$

Since

$$g^{a^\dagger a}|\alpha\rangle = e^{(g^2-1)|\alpha|^2/2}|g\alpha\rangle, \tag{6.14}$$

we can simplify this by letting $K = L g^{a^\dagger a}$. The result,

$$L|g\alpha\rangle = |g\alpha\rangle\frac{\langle g\alpha|P_N L|g\alpha\rangle}{\mu}, \tag{6.15}$$

says that $|g\alpha\rangle$ is an eigenstate of L. Since the coherent states on a circle are a basis for the Hilbert space, this determines L to be a function of the annihilation operator a. The rotational symmetry further requires that L have number-state matrix elements on only one diagonal strip, implying that $L = \lambda a^k$, where k is a non-negative integer and λ can be taken to be real without loss of generality.

The possible optimal Kraus operators are

$$\begin{aligned} K_k &= \lambda a^k g^{a^\dagger a} = \lambda g^{a^\dagger a}(ga)^k \\ &= \lambda \sum_{n=0}^{\infty} g^{n+k}\sqrt{\frac{(n+k)!}{n!}}|n\rangle\langle n+k|, \\ k &= 0,1,2,\ldots. \end{aligned} \tag{6.16}$$

This operator has nonzero matrix elements only on the kth diagonal strip above the main diagonal. It is not surprising that this class of operators emerges, because they do take $|\alpha\rangle$

to a multiple of $|g\alpha\rangle$, just as we would like an immaculate amplifier to do. The success probability and fidelity become

$$p(\checkmark|\bar{\alpha}) = \lambda^2 g^{2k} e^{(g^2-1)\bar{\alpha}^2} \bar{\alpha}^{2k} \langle g\alpha|P_N|g\alpha\rangle, \quad (6.17)$$

$$F(\bar{\alpha}) = \langle g\alpha|\, P_N\, |g\alpha\rangle = e^{-g^2\bar{\alpha}^2} e_N(g^2\bar{\alpha}^2) = \mu. \quad (6.18)$$

We can increase the success probability without changing the fidelity by letting λ^2 increase, but there is a limit to this increase set by the requirement that

$$I \geqslant K_k^\dagger P_N K_k = \lambda^2 \sum_{n=0}^{N} g^{2(n+k)} \frac{(n+k)!}{n!} |n+k\rangle\langle n+k|. \quad (6.19)$$

Since the eigenvalues increase with n, the constraint is set by the largest eigenvalue ($n = N$). Choosing the largest possible value,

$$\lambda^2 = \frac{N!}{(N+k)!} \frac{1}{g^{2(N+k)}}, \quad (6.20)$$

maximizes the success probability.

The final results of these considerations are the Kraus operators

$$K_k = \sqrt{\frac{N!}{(N+k)!}} \frac{a^k g^{a^\dagger a}}{g^{N+k}} = \sqrt{\frac{N!}{(N+k)!}} \frac{g^{a^\dagger a} a^k}{g^N} \quad (6.21)$$

and the corresponding success probability and fidelity,

$$p(\checkmark|\bar{\alpha}) = \frac{N!}{(N+k)!} \frac{e^{-\bar{\alpha}^2}\bar{\alpha}^{2k}}{g^{2N}} e_N(g^2\bar{\alpha}^2), \quad (6.22)$$

$$F(\bar{\alpha}) = e^{-g^2\bar{\alpha}^2} e_N(g^2\bar{\alpha}^2). \quad (6.23)$$

Equation (6.23) was derived by Fiurášek [8] (our amplitude gain g is his $\sqrt{M}$) by maximizing an average fidelity. Fiurášek considers a Gaussian distribution of input coherent states. His average fidelity includes, first, an average over the success probability, normalized to an average success probability, averaged over the input Gaussian, and, second, an average over the input Gaussian. He does not quote the probability of success, and he only finds the $k = 0$ case. He formulates the optimization problem as a semidefinite program, whereas we use a simple Lagrange-multiplier maximization.

It is useful to pause here to summarize properties of the fidelity and the success probability. The fidelity (6.23) is the probability of the first $N+1$ number states in the Poisson distribution associated with the coherent state $|g\alpha\rangle$. As we anticipated, this fidelity is close to 1 for $g\bar{\alpha} \ll \sqrt{N}$, goes to zero for $g\bar{\alpha} \gg \sqrt{N}$, and transitions between these two extremes around $g\bar{\alpha} \simeq \sqrt{N}$. Indeed, we can use the Chernoff bound for the probability in the tails of a Poisson distribution with mean $g^2\bar{\alpha}^2$ to bound the fidelity in the two extremes [40],

$$g^2\bar{\alpha}^2 \leqslant N: \quad F(\bar{\alpha}) = 1 - \Pr[\, n \geqslant N+1|g^2\bar{\alpha}^2\,] \geqslant 1 - e^{-g^2\bar{\alpha}^2} \left(\frac{eg^2\bar{\alpha}^2}{N+1}\right)^{N+1}, \quad (6.24)$$

$$g^2\bar{\alpha}^2 > N: \quad F(\bar{\alpha}) = \Pr[\, n \leqslant N|g^2\bar{\alpha}^2\,] \leqslant \left(\frac{eg^2\bar{\alpha}^2 e^{-g^2\bar{\alpha}^2/N}}{N}\right)^N. \quad (6.25)$$

The width of the transition region can be estimated by remembering that the two-standard-deviation phase-plane radius of a coherent state is 1. As a consequence, the amplified output begins to contact the number state cutoff at N when $g\bar{\alpha} + 1 \simeq \sqrt{N}$ and leaves the high-fidelity region entirely when $g\bar{\alpha} - 1 \simeq \sqrt{N}$. Thus, we expect the transition from unity fidelity to zero fidelity to occur as $\bar{\alpha}$ varies from $(\sqrt{N}-1)/g$ to $(\sqrt{N}+1)/g$.

The fidelity does not depend on k, but the success probability does, so the value of k that maximizes the success probability can change as $\bar{\alpha}$ changes. The amplifier map (6.1) cannot depend, of course, on the input amplitude, so we must settle on a value of k and apply the resulting map to all input coherent states. We are most interested in the high-fidelity regime, where the leading-order behavior of the success probability (6.22) is

$$p(\checkmark|\bar{\alpha}) = \frac{N!}{(N+k)!} \frac{e^{-\bar{\alpha}^2}\bar{\alpha}^{2k}}{g^{2N}}, \quad \bar{\alpha} \ll \sqrt{N}/g. \quad (6.26)$$

In this regime all values of k have success probabilities that are exponentially small in N, but $k = 0$ is the best of a sad lot, indicating that it is the best value of k. Before investigating the different values of k in detail, however, we extend the Kraus operator $P_N K_k$ so that it can map outside S_N in a way that increases the fidelity and success probability.

The extension we seek should preserve the phase insensitivity of $P_N K_k$ and should not interfere with the output of $P_N K_k$ in the subspace S_N. A glance at Eq. (6.16) shows that the extension must have the form $\Upsilon_k = P_N K_k + \sum_{n=N+1}^{\infty} \upsilon_n\, |n\rangle\, \langle n+k|$. Now we impose the condition

$$I \geqslant \Upsilon_k^\dagger \Upsilon_k = K_k^\dagger P_N K_k + \sum_{n=N+1}^{\infty} |\upsilon_n|^2\, |n+k\rangle\, \langle n+k|\,. \quad (6.27)$$

The term $K_k^\dagger P_N K_k$ already satisfies the inequality in the subspace S_{N+k} spanned by the first $N+k+1$ number states [see Eq. (6.19)], and we can maximize the amplifier's success probability by saturating the inequality for the second term, i.e., by choosing $\upsilon_n = 1$ for $n = N+1, N+2, \ldots$, with the result that

$$\Upsilon_k = P_N K_k + \sum_{n=N+1}^{\infty} |n\rangle\, \langle n+k|\,. \quad (6.28)$$

With this choice, notice that for $k = 0$, the additional term in Υ_k is simply the unit operator in the orthocomplement of S_N.

The extension of the Kraus operator has essentially no impact on the operation of the amplifier in the high-fidelity input region. It does increase the fidelity marginally in the transition region by including in the output number-state components with $n > N$. The biggest effect is to increase dramatically the success probability in the low-fidelity regime beyond $\bar{\alpha} \simeq \sqrt{N+k}$, but this improvement is a pyrrhic victory: All it does is to allow the amplifier to report that it worked on inputs where the output has essentially the same fidelity with the target as the input does.

Using the extended Kraus operators to calculate the success probability and the fidelity of the output with the target

$|g\alpha\rangle$ gives

$$p_k(\checkmark|\bar{\alpha}) = \langle\alpha|\,\Upsilon_k^\dagger\Upsilon_k\,|\alpha\rangle = e^{-\bar{\alpha}^2}\bar{\alpha}^{2k}\left(\frac{N!}{(N+k)!}\frac{1}{g^{2N}}e_N(g^2\bar{\alpha}^2) + \sum_{n=N+1}^{\infty}\frac{\bar{\alpha}^{2n}}{(n+k)!}\right), \tag{6.29}$$

$$F_k(\bar{\alpha}) = \frac{|\langle g\alpha|\Upsilon_k|\alpha\rangle|^2}{p_k(\checkmark|\alpha)} = \frac{e^{-g^2\bar{\alpha}^2}}{p_k(\checkmark|\bar{\alpha})/e^{-\bar{\alpha}^2}\bar{\alpha}^{2k}}\left(\sqrt{\frac{N!}{(N+k)!}}\frac{1}{g^N}e_N(g^2\bar{\alpha}^2) + \sum_{n=N+1}^{\infty}\frac{g^n\bar{\alpha}^{2n}}{\sqrt{n!(n+k)!}}\right)^2. \tag{6.30}$$

With the extended Kraus operators, both the success probability and the fidelity depend on k. In the high-fidelity regime, $\bar{\alpha} \ll \sqrt{N}/g$, the extension terms have little impact: The fidelity limits to unity, and the success probability has the form given in Eq. (6.26), which decreases exponentially with N. For $\bar{\alpha} \gg \sqrt{N}/g$, the fidelity goes to zero much as it did before. The success probability, however, has a new transition that occurs at $\bar{\alpha}^2 \simeq N + k$: For $\bar{\alpha}^2 \gg N + k$, only the extension term matters, so the success probability becomes nearly the entire probability under a Poisson distribution with mean $\bar{\alpha}^2$, i.e., $p_k(\checkmark|\bar{\alpha}) = \Pr[\,n \geqslant N + k + 1|\bar{\alpha}^2\,]$, and this limits to unity as $\bar{\alpha}^2 \to \infty$.

To gain insight into the success probability (6.29) and output fidelity (6.30), we plot them in Fig. 5 as a function of the input amplitude $\bar{\alpha}$ for $k = 0$, 1, and 2. In Fig. 5(a), we take an amplitude gain $g = \sqrt{2}$ and $N = 4$, both of which are too small to see some of the characteristic features we have discussed. The three fidelity curves are approximately unity until $\bar{\alpha} \sim \sqrt{N}/g$. After this point the fidelity decreases to zero. Conversely, the three success-probability curves start close to zero and rise to unity after $|\alpha| \sim \sqrt{N}/g$. Figure 5(b) plots the same curves for $g = 3$ and $N = 9$, values big enough to see the characteristic features of the two quantities. In particular, it is apparent that the fidelity transitions from unity fidelity to zero fidelity around $\bar{\alpha} \simeq \sqrt{N}/g = 1$, with the transition occurring between $(\sqrt{N} - 1)/g = 2/3$ and $(\sqrt{N} + 1)/g = 4/3$, as anticipated. For all three values of k, the success probability in panel (c) rises from its initial small value to unity, with the rise occurring around the second transition at $\bar{\alpha} \simeq \sqrt{N}$.

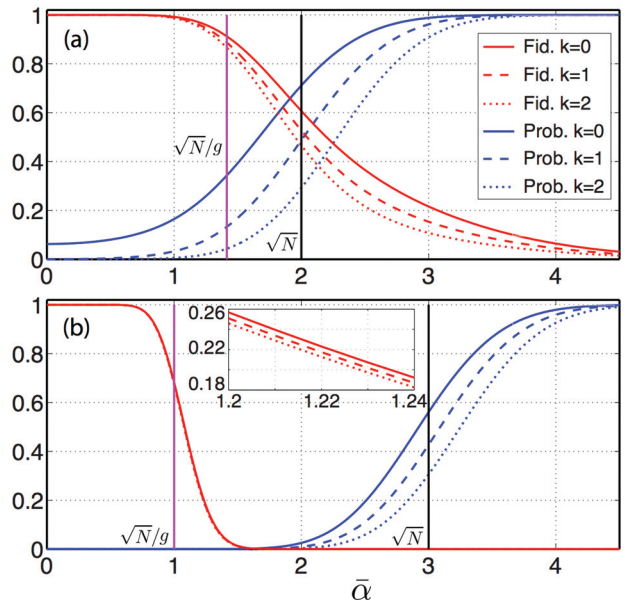

FIG. 5. (Color online) Fidelity $F_k(\bar{\alpha})$ of Eq. (6.30) (descending curves) and success probability $p_k(\checkmark|\bar{\alpha})$ of Eq. (6.29) (ascending curves) plotted as functions of input amplitude $\bar{\alpha}$ for different extended Kraus operators Υ_k with $k = 0$ (solid lines), 1 (dashed lines), and 2 (dotted lines): (a) $g = \sqrt{2}$, $N = 4$; (b) $g = 3$, $N = 9$. The inset in (b) illustrates the small differences in fidelity, undetectable in the main plot, among the three values of k.

It turns out that the success probability and fidelity for any value of k are bounded in the following way:

$$0 \leqslant p_k(\checkmark|\bar{\alpha}) \leqslant p_0(\checkmark|\bar{\alpha}), \tag{6.31}$$

$$F_k(\bar{\alpha}) \leqslant F_0(\bar{\alpha}). \tag{6.32}$$

These bounds are illustrated by the examples plotted in Fig. 5, and we have proven them analytically. The proof, which is tedious, is contained in Appendix C. The bounds confirm that the best value of k is $k = 0$. We also show in Appendix C that

$$F_0(\bar{\alpha}) \geqslant \langle g\alpha|P_N|g\alpha\rangle, \tag{6.33}$$

which indicates that the $k = 0$ extension increases the fidelity over that of the restricted Kraus operators.

If the amplifier quantum operation has Kraus operators other than Υ_0, our analysis shows that these other Kraus operators necessarily reduce the fidelity and the success probability. This justifies our earlier assumption of a single Kraus operator. The best Kraus operator is Υ_0, and this gives an amplifier quantum operation $\mathcal{A}_N = \Upsilon_0 \odot \Upsilon_0^\dagger$.

The three plots in Fig. 6, all for $k = 0$, have different values of g and N, but roughly the same high-fidelity input region: The ratio $\sqrt{N}/g = 1$ in panels (a) and (c), whereas in (b) it is $\sqrt{2}$. The plots include the fidelity and success probability coming from the extended Kraus operator Υ_0 and, for comparison, the fidelity and success probability coming from the restricted Kraus operator $P_N K_0$. Panels (a) and (b) are interesting because they have gains typical of that achieved in experiments, but the transitions are not very sharp, g and N being too small to see the characteristic features of the plotted quantities. In panel (c), where $g = 3$ and $N = 9$, the characteristic features emerge: The extended Kraus operator provides a small increase in fidelity through the transition region; the success probability using Υ_0 ascends to 1 beyond $\bar{\alpha} \simeq \sqrt{N}$, instead of falling back to nearly zero, as happens with the success probability that comes from $P_N K_0$. These plots illustrate the superior qualities of the extended Kraus operator Υ_0; we do not consider the restricted Kraus operators again.

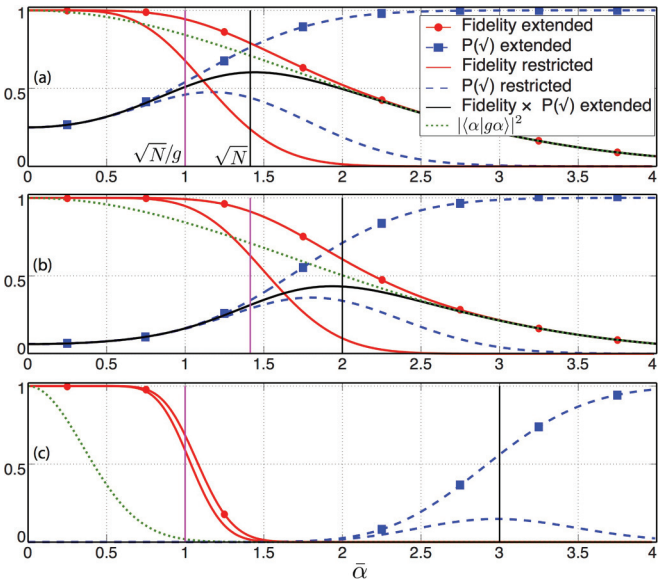

FIG. 6. (Color online) Fidelity $F_0(\bar{\alpha})$ using the extended Kraus operator Υ_0 [Eq. (6.30)] (solid line with solid circles); corresponding success probability $p_0(\checkmark|\bar{\alpha})$ [Eq. (6.29)] (dashed line with solid squares); fidelity $F(\bar{\alpha})$ using the restricted Kraus operator $P_N K_0$ [Eq. (6.23)] (solid descending line); corresponding restricted success probability $p(\checkmark|\bar{\alpha})$ [Eq. (6.22) with $k = 0$] (dashed line); probability-fidelity product $p_0(\checkmark|\bar{\alpha})F_0(\bar{\alpha})$ (solid humped line); and overlap $|\langle\alpha|g\alpha\rangle|^2$ (dotted line), all plotted as functions of input amplitude $\bar{\alpha}$: (a) $g = \sqrt{2}$, $N = 2$; (b) $g = \sqrt{2}$, $N = 4$; (c) $g = 3$ $N = 9$.

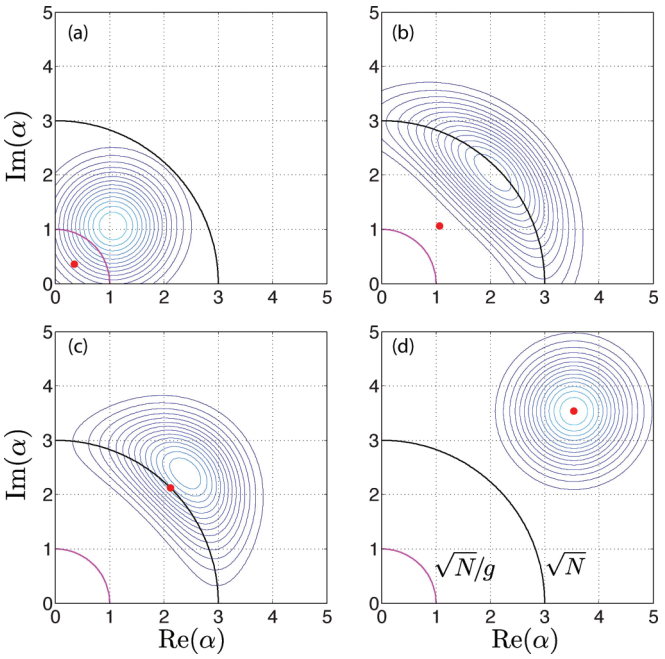

FIG. 7. (Color online) Q distribution of the output state of the immaculate linear amplifier given by the extended Kraus operator Υ_0, with $g = 3$ and $N = 9$, for four amplitudes of input coherent state: (a) $\bar{\alpha} = 0.5$, (b) $\bar{\alpha} = 1.5$, (c) $\bar{\alpha} = 3$, (d) $\bar{\alpha} = 5$. The (red) dot denotes the center of the input coherent state. The transition at input radius $\sqrt{N}/g = 1$ is marked by a (red) arc, and its image at the output by the (black) arc at radius $\sqrt{N} = 3$. Thus (a) lies within the high-fidelity region, and the output looks like an amplified coherent state; (b) lies beyond the transition, and its output is flattened along the arc of radius $\sqrt{N}$. A second transition occurs near $\bar{\alpha} \simeq \sqrt{N}$, as Υ_0 transitions to being the identity operator. Thus (c), lying right in the middle of this second transition, has output that is little amplified and is flattened along the radial direction, whereas (d), lying well beyond the second transition, has output that is nearly identical to the input coherent state.

Figure 6 plots two other quantities: the probability-fidelity product, $p_0(\checkmark|\bar{\alpha})F_0(\bar{\alpha}) = |\langle g\alpha|\Upsilon_0|\alpha\rangle|^2$, for our phase-insensitive immaculate amplifier and the overlap $|\langle\alpha|g\alpha\rangle|^2 = e^{-(g-1)^2\bar{\alpha}^2}$. The latter can be regarded as the fidelity against the target state of a device that does nothing, i.e., outputs the input. Since nothing can be done with unit probability, $|\langle\alpha|g\alpha\rangle|^2$ is also the probability-fidelity product for a device that does nothing. A minimal requirement for a useful amplifier is that it be better than doing nothing. The plots suggest that, as far as the probability-fidelity product is concerned, the phase-insensitive immaculate amplifier is never better than doing nothing—indeed, $|\langle g\alpha|\Upsilon_0|\alpha\rangle|^2 \leqslant |\langle g\alpha|\alpha\rangle|^2$ follows immediately from the fact that Υ_0 is diagonal in the number basis with positive eigenvalues bounded above by 1—and approaches that standard only for $\bar{\alpha} \gtrsim \sqrt{N}$, where, as we have already seen, Υ_0 becomes the identity map. For comparison, the probability-fidelity product for an ideal linear amplifier is $1/g^2$ [see Eq. (2.23)], which beats the do-nothing standard for $\bar{\alpha}^2 \geqslant \ln g^2/(g-1)^2$.

The key features of the output state of the immaculate amplifier $\mathcal{A}_N = \Upsilon_0 \odot \Upsilon_0$ are illustrated by the Q-distribution plots in Fig. 7. In Fig. 7(a), an input state within the high-fidelity input region is transformed to an output state that is very close to the target output coherent state. In panel (b), however, the input state is beyond the high-fidelity input region; the output state gets plastered against the output arc of radius $\sqrt{N}$, producing a flattening and distortion along this arc. This distortion is very much like that seen in experiments that implement immaculate linear amplification [28,29,32–34]. (It is worth noting that for the unextended Kraus operator $P_N K_0$, as $\bar{\alpha}$ increases beyond $\sqrt{N}/g$, the output state becomes essentially the Fock state $|N\rangle$.) Panels (c) and (d) illustrate the passage through the second transition at $\bar{\alpha} \simeq \sqrt{N}$, as the action of Υ_0 transitions to being that of the unit operator.

In Fig. 8 we plot the SNR-based performance measure defined in Sec. II C, with the key difference that we have two such SNRs: $\mathrm{SNR}_1 = \langle x_1\rangle/\delta x_1 = \sqrt{2}\bar{\alpha}/\delta x_1$ for the amplitude (radial) quadrature x_1 and $\mathrm{SNR}_2 = \langle x_1\rangle/\delta x_2$ for the phase quadrature x_2 ($\langle x_2\rangle = 0$). As in Sec. II C, the uncertainties in the SNRs are calculated using antinormal ordering, which applies when one intends to measure both quadratures [43]. Figure 8 plots the SNR quantities for an input coherent state $|\alpha\rangle$, the target output state $|g\alpha\rangle$, and the output of an Υ_0 immaculate amplifier. As discussed in Sec. II C, the right way to take into account the success probability of the immaculate amplifier is to multiply the SNRs by the square root of the working probability; thus Fig. 8 also shows plots the root-probability–SNRs, $\sqrt{p_0(\checkmark|\bar{\alpha})}\mathrm{SNR}_1$ and $\sqrt{p_0(\checkmark|\bar{\alpha})}\mathrm{SNR}_2$ for the output of the immaculate amplifier.

Panel (a) of Fig. 8 plots these quantities for a gain typical of that achieved in experiments. Panel (b) has a larger gain that shows the characteristic features of these quantities. Within

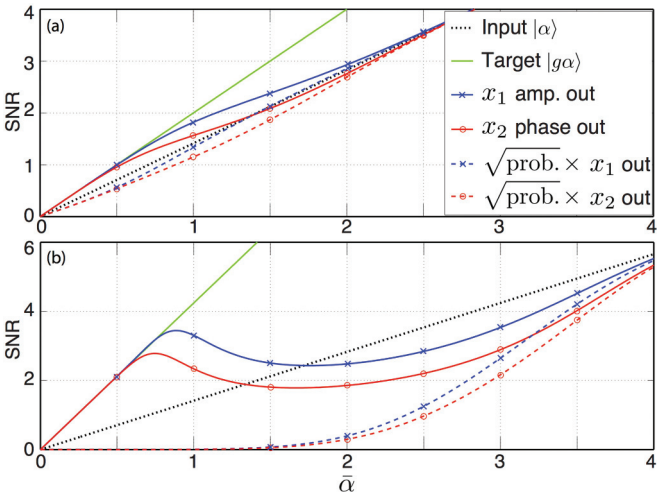

FIG. 8. (Color online) Antinormally ordered quadrature SNRs as a function of the input amplitude $\bar{\alpha}$. The SNR is defined as $\text{SNR}_1 = \langle x_1 \rangle / \delta x_1$ for the amplitude (radial) quadrature x_1 or as $\text{SNR}_2 = \langle x_1 \rangle / \delta x_2$ for the phase quadrature x_2. Four of the plots are for (i) the input state $|\alpha\rangle$ (dotted line), for which $\text{SNR}_1 = \text{SNR}_2$ [this is also the bound given in Eq. (2.21)]; (ii) the output target state $|g\alpha\rangle$ (solid line), for which $\text{SNR}_1 = \text{SNR}_2$; and (iii) and (iv) the output state of the Υ_0 immaculate amplifier (SNR_1, solid line with crosses; SNR_2, solid line with circles). The other two plots give the amplifier SNRs multiplied by the square root of the working probability, $\sqrt{p_0(\surd|\bar{\alpha})}$, as described in the text: The dashed line with crosses plots $\sqrt{p_0(\surd|\bar{\alpha})}\text{SNR}_1$, and the dashed line with circles plots $\sqrt{p_0(\surd|\bar{\alpha})}\text{SNR}_2$. For the amplifier plots, (a) has $g = \sqrt{2}$, $N = 2$, and (b) has $g = 3$, $N = 9$.

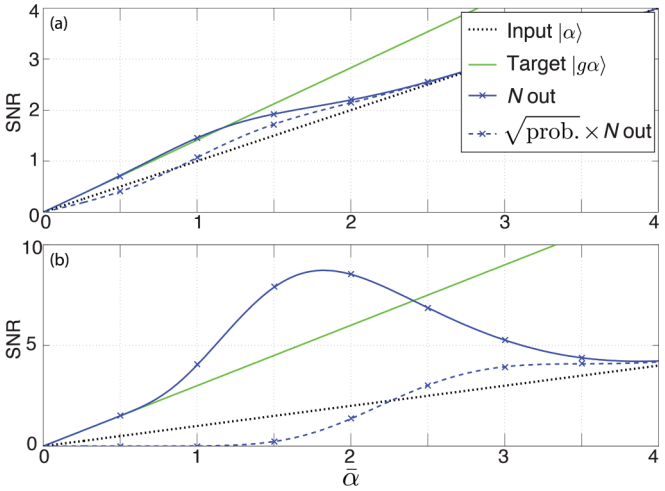

FIG. 9. (Color online) Number-based SNR measure as a function of the input amplitude $\bar{\alpha}$. The four plots are SNR_N for the input state $|\alpha\rangle$ (dotted line); SNR_N for the output target state $|g\alpha\rangle$ (solid line); SNR_N for the output state of the Υ_0 immaculate amplifier (solid line with crosses); and the root-probability–SNR measure $\sqrt{p_0(\surd|\bar{\alpha})}\text{SNR}_N$ for the output state of the Υ_0 immaculate amplifier (dashed line with crosses). For the amplifier plots, (a) has $g = \sqrt{2}$, $N = 2$, and (b) has $g = 3$, $N = 9$.

the high-fidelity input region, the output SNRs of the amplifier match those of the target output state, but they fall away from the target as $\bar{\alpha}$ moves out of the high-fidelity region. The root-probability–SNRs show that once the success probability is taken into account, the immaculate amplifier does not do as well as the input coherent state; it always satisfies the bound (2.21) and is not even close to the bound in the high-fidelity region.

One could use other SNR-based performance measures, an example being one based on the statistics of number of quanta. Doing this can lead to different conclusions. In Fig. 9, we consider a number-based SNR defined as $\text{SNR}_N = \langle N \rangle / \Delta N$, where $N = a^\dagger a$ is the number operator and ΔN is the uncertainty in N. Figure 9 shows that, in terms of SNR_N, first, the output of the immaculate amplifier can do better than the target output state and, second, the number-based root-probability–SNR, which includes the square root of the success probability, can exceed that of the input coherent state. The first of these improvements seems to arise from the distortion of the output state as it leaves the high-fidelity region at $\bar{\alpha} \simeq \sqrt{N}/g$, which is 1 in both plots; this distortion amounts to squeezing in the radial direction, as is illustrated in Fig. 7(b). The second improvement is due to the same distortion, but is also aided by the increase in success probability, displayed in Fig. 6, for $\bar{\alpha} \gtrsim \sqrt{N}$. Since these improvements arise from effects outside the region of high-fidelity immaculate amplification, they seem to be incidental to the operation of the device as an immaculate amplifier.

We conclude this section by reiterating that in the high-fidelity regime, the $k = 0$ extended-Kraus-operator immaculate amplifier has a success probability [see Eq. (6.26) with $k = 0$]

$$p_0(\surd|\bar{\alpha}) = \frac{e^{-\bar{\alpha}^2}}{g^{2N}}. \tag{6.34}$$

This can be regarded as the chief result of this section: Within the high-fidelity region of operation, an approximate phase-insensitive immaculate linear amplifier has a success probability that decreases exponentially with the size N/g^2 of the high-fidelity input region, with the base of the exponential being g^{2g^2}. This result, for the optimal phase-insensitive immaculate amplifier, indicates that the very low success probabilities seen in experiments [25,28,29], though they might be depressed yet further by technical difficulties, are an unavoidable consequence of trying to perform phase-insensitive immaculate amplification.

VII. CONCLUSION

Immaculate amplification is an attempt to evade the uncertainty principle. Our chief conclusion is that immaculate amplifiers, if they operate phase-insensitively, cannot achieve both high fidelity to the target output state and even reasonably high working probability. Indeed, in phase-plane regions where a phase-insensitive device amplifies immaculately with high fidelity, the probability that the device works is extremely small. The small working probabilities seen in experiments that implement immaculate amplification are not solely a consequence of technical imperfections; they are inherent in the nature of phase-insensitive immaculate amplification.

We suggest several changes in focus that might reconcile the concept of immaculate amplification and quantum theory,

as well as leading to more positive results than those reported here. The first of these is simple: Phase-insensitive immaculate amplification, with its reduction in noise from input to output, might be a step too far; perhaps a better sort of device to seek is a probabilistic perfect amplifier, which would amplify the symmetrically ordered input noise without adding the noise of a (deterministic) ideal linear amplifier. Working probabilities for probabilistic perfect amplifiers might be better than those we have found for immaculate amplifiers.

The second change is to abandon hope for invariance under phase-plane rotations and of working on more than one circle of input coherent states, focusing instead on the quite encouraging probabilities we have found for immaculate amplification of sparse collections of coherent states on a single input circle. Nondeterministic devices have found many uses in quantum information science, a notable example being the KLM scheme for linear-optical quantum computing [44]. Immaculate amplifiers, like the one described formally by Eq. (5.35), which are both phase sensitive and amplitude specific, can work on sparse collections of coherent states with high success probability; they might find application in problems such as discrimination of the coherent states used in phase-shift keying [11,12]. There are important questions regarding communications protocols based on such devices: How robust are they against amplitude and phase noise in the preparation of the input coherent states? How badly are rates impacted by the success probability? These questions are certainly worth investigating.

Finally, we suggest a change in the quantum-information-science approach to analyzing amplifying devices. The literature on immaculate amplification has focused on the fidelity of the output with the immaculate target. We have stressed that fidelity cannot be considered as a performance measure alone; the probability-fidelity product is a better measure of overall performance. Instead of attempting to optimize the probability-fidelity product, however, it might be better to develop performance measures suited to specific applications. For metrological applications, the root-probability–SNR impresses us as an appropriate measure of performance. Continuous-variable quantum key distribution is a communication protocol that might use immaculate amplification and where key rates are an obvious performance measure. Some steps have been taken to optimize key rates in this context [45,46], but more work is needed. To paraphrase Emerson, a foolish fidelity to fidelity is the hobgoblin of small minds [48]; that is, each application begs for its own performance measure.

ACKNOWLEDGMENTS

The authors thank S. Croke, A. Denney, F. Ferreyrol, M. J. W. Hall, S. Kocsis, A. P Lund, I. Marvian, G. J. Pryde, R. W. Spekkens, T. C. Ralph, and N. Walk for helpful and enlightening conversations and email exchanges. This work was supported in part by National Science Foundation Grants No. PHY-1212445 and No. PHY-1005540 and by Office of Naval Research Grant No. N00014-11-1-0082. J.C. and C.M.C. also acknowledge support by the National Science Foundation under Grant No. NSF PHY-1125915 at the Kavli Institute for Theoretical Physics.

APPENDIX A: LINEAR DEPENDENCE OF COHERENT STATES ON A CIRCLE

We review the linear dependence of the continuum of coherent states on a phase-space circle of radius $\bar{\alpha}$ centered at the origin. The reader should also consult the appendix of Ref. [36].

A coherent state is represented in the number basis by

$$|\alpha = \bar{\alpha}e^{i\phi}\rangle = e^{-\bar{\alpha}^2/2}\sum_{n=0}^{\infty}\frac{\bar{\alpha}^n e^{in\phi}}{\sqrt{n!}}\,|n\rangle\,. \tag{A1}$$

The coherent states $|\bar{\alpha}e^{i\phi}\rangle$, $0 \leqslant \phi < 2\pi$, on a circle of radius $\bar{\alpha}$ are complete, but they are not linearly independent.

These states are linearly dependent, as we can see from

$$\int_0^{2\pi}\frac{d\phi}{2\pi}\,e^{-in\phi}|\bar{\alpha}e^{i\phi}\rangle = \begin{cases} e^{-\bar{\alpha}^2/2}\,\frac{\bar{\alpha}^n}{\sqrt{n!}}|n\rangle, & n \geqslant 0, \\ 0, & n < 0. \end{cases} \tag{A2}$$

The vanishing of the integral for $n < 0$ shows that the states are not linearly independent.

That these states are complete follows immediately from expanding any vector as

$$|\psi\rangle = \sum_{n=0}^{\infty}|n\rangle\langle n|\psi\rangle = \int\frac{d\phi}{2\pi}\,\chi(\phi)|\bar{\alpha}e^{i\phi}\rangle, \tag{A3}$$

where the function $\chi(\phi)$ has Fourier representation

$$\chi(\phi) = \sum_{n=0}^{\infty}\chi_n e^{-in\phi}, \tag{A4}$$

with the positive Fourier coefficients uniquely determined to be

$$\chi_n = e^{\bar{\alpha}^2/2}\frac{\sqrt{n!}}{\bar{\alpha}^n}\langle n|\psi\rangle, \quad n > 0, \tag{A5}$$

and the negative Fourier coefficients arbitrary. That the negative Fourier coefficients can be changed arbitrarily without changing $|\psi\rangle$ expresses the linear dependence of the coherent states on a circle.

APPENDIX B: ROTATIONALLY SYMMETRIC QUANTUM OPERATIONS

The superoperator that effects a rotation by θ in the phase plane is

$$\mathcal{R}(\theta) = e^{i\theta a^\dagger a}\odot e^{-i\theta a^\dagger a} = \sum_{n,m}e^{i(n-m)\theta}|n\rangle\langle n|\odot|m\rangle\langle m|. \tag{B1}$$

A quantum operation $\mathcal{A}$ is invariant under rotations if it commutes with $\mathcal{R}(\theta)$ for all θ, i.e., $\mathcal{R}(\theta)\circ\mathcal{A} = \mathcal{A}\circ\mathcal{R}(\theta)$. The symmetry condition implies that $\mathcal{A}$ has the form

$$\mathcal{A} = \sum_k\sum_{n,m}A^{(k)}_{nm}|n+k\rangle\langle n|\odot|m\rangle\langle m+k|. \tag{B2}$$

That $\mathcal{A}$ is a quantum operation, i.e., is completely positive, implies that $A^{(k)}$ is a positive Hermitian matrix and thus can be diagonalized by a unitary matrix:

$$A^{(k)}_{nm} = \sum_l\lambda^{(k)}_l U_{nl}U^{(k)*}_{ml}. \tag{B3}$$

This brings $\mathcal{A}$ into the form

$$\mathcal{A} = \sum_{k,l} M_l^{(k)} \odot M_l^{(k)\dagger}, \tag{B4}$$

where the operators

$$M_l^{(k)} = \sum_n \sqrt{\lambda_l^{(k)}} U_{nl}^{(k)} |n+k\rangle\langle n| \tag{B5}$$

are orthogonal Kraus operators. Invariance under rotations manifests itself as the requirement that these Kraus operators have nonzero number-basis matrix elements only in one diagonal strip specified by the integer k.

APPENDIX C: OPTIMAL SUCCESS PROBABILITY AND FIDELITY

In this Appendix we show that the success probabilities and fidelities of Eqs. (6.29) and (6.30) satisfy the bounds (6.31)–(6.33).

We first show the inequalities

$$p_k(\checkmark|\bar{\alpha}) \geqslant p_{k+1}(\checkmark|\bar{\alpha}), \tag{C1}$$

$$F_k(\bar{\alpha}) \geqslant F_{k+1}(\bar{\alpha}); \tag{C2}$$

from these, we can also conclude that $p_k(\checkmark|\bar{\alpha})F_k(\bar{\alpha}) \geqslant p_{k+1}(\checkmark|\bar{\alpha})F_{k+1}(\bar{\alpha})$. This proves that the best success probability and fidelity are achieved at $k=0$, i.e., by the Kraus operator Υ_0.

The success-probability inequalities (C1) follow straightforwardly from the difference

$$\begin{aligned} Q_k &= \Upsilon_k^\dagger\Upsilon_k - \Upsilon_{k+1}^\dagger\Upsilon_{k+1} \\ &= \frac{N!}{(N+k)!}\frac{1}{g^{2N}}\sum_{n=0}^{N}\frac{(n+k)!}{n!}g^{2n}\left(1-\frac{n}{N+k+1}\frac{1}{g^2}\right) \\ &\quad\times |n+k\rangle\langle n+k| \geqslant 0. \end{aligned} \tag{C3}$$

The manifest positivity of Q_k means that $\langle\alpha|Q_k|\alpha\rangle \geqslant 0$, which is the inequality (C1).

To show the fidelity inequalities (C2), we begin by writing Kraus operator (6.28) in the form

$$\Upsilon_k = \sum_{n=0}^{\infty} f_k(n)\sqrt{\frac{(n+k)!}{n!}}|n\rangle\langle n+k|, \tag{C4}$$

where

$$f_k(n) = \begin{cases} \sqrt{\frac{N!}{(N+k)!}}\frac{g^n}{g^N}, & n=0,\ldots,N, \\ \sqrt{\frac{n!}{(n+k)!}}, & n=N+1,N+2,\ldots. \end{cases} \tag{C5}$$

Notice that $f_k(n)$ does not decrease with n for $n \leqslant N$, reaches it maximum value at $n=N$, and then is a nonincreasing function of n for $n \geqslant N$.

Using $f_k(n)$, we can write

$$\langle g\alpha|\Upsilon_k|\alpha\rangle = e^{-(g^2-1)\bar{\alpha}^2/2}\alpha^k \mathrm{E}[g^n f_k(n)], \tag{C6}$$

where E denotes an expectation value with respect to the Poisson distribution $\Pr[n|\bar{\alpha}^2] = |\langle n|\alpha\rangle|^2 \equiv P_n$. We also have

$$p_k(\checkmark|\bar{\alpha}) = \langle\alpha|\Upsilon_k^\dagger\Upsilon_k|\alpha\rangle = \bar{\alpha}^{2k}\mathrm{E}\big[f_k^2(n)\big]. \tag{C7}$$

Thus, the fidelity (6.30) can be put in the form

$$F_k(\bar{\alpha}) = e^{-(g^2-1)|\alpha|^2}\frac{(\mathrm{E}[g^n f_k(n)])^2}{\mathrm{E}\big[f_k^2(n)\big]}. \tag{C8}$$

For any $k=0,1,\ldots,$ we define

$$\begin{aligned} h_k(n) &\equiv \frac{f_{k+1}(n)}{f_k(n)} \\ &= \begin{cases} \frac{1}{\sqrt{N+k+1}}, & n=0,\ldots,N, \\ \frac{1}{\sqrt{n+k+1}}, & n=N+1, \quad N+2,\ldots. \end{cases} \end{aligned} \tag{C9}$$

Notice that $h_k(n)$ is a nonincreasing function of n.

The fidelity inequality (C2) equivalent to

$$\begin{aligned} \mathrm{LHS} &= (\mathrm{E}[g^n f_{k+1}(n)])^2\mathrm{E}\big[f_k^2(n)\big] \\ &\leqslant (\mathrm{E}[g^n f_k(n)])^2\mathrm{E}[f_{k+1}(n)^2] = \mathrm{RHS}. \end{aligned} \tag{C10}$$

Since, by the Schwarz inequality,

$$\mathrm{LHS} \leqslant \mathrm{E}[g^n f_k(n)]\mathrm{E}\big[g^n f_k(n)h_k^2(n)\big]\mathrm{E}\big[f_k^2(n)\big] \equiv \mathcal{I}, \tag{C11}$$

we can achieve our objective by showing that $\mathcal{I} \leqslant \mathrm{RHS}$ or, equivalently, that

$$\mathrm{E}\big[g^n f_k(n)h_k^2(n)\big]\mathrm{E}\big[f_k^2(n)\big] \leqslant \mathrm{E}[g^n f_k(n)]\mathrm{E}\big[f_{k+1}^2(n)\big]. \tag{C12}$$

Equation (C12) can be written as

$$0 \geqslant \sum_{m,n} G(m,n) = \sum_{n=0}^{\infty}\sum_{m=0}^{n-1} G(m,n) + G(n,m), \tag{C13}$$

where

$$G(m,n) = P_n P_m f_k(n) f_k(m) h_k^2(m)[g^m f_k(n) - g^n f_k(m)]. \tag{C14}$$

In the final form of Eq. (C13), we use the fact that $G(n,n)=0$ to exclude the terms along the diagonal from the sum. Now what we show is that

$$\begin{aligned} &G(m,n) + G(n,m) \\ &\quad = P_n P_m f_k(n) f_k(m)[g^m f_k(n) - g^n f_k(m)]\big[h_k^2(m) - h_k^2(n)\big] \end{aligned} \tag{C15}$$

is never positive for $n > m$. There are three cases to consider. First, when $m < n \leqslant N$, $h_k(m) = h_k(n)$, so the quantity (C15) vanishes. Second, when $m \leqslant N < n$, $h_k(m) \geqslant h_k(n)$ and

$$g^m f_k(n) - g^n f_k(m) = g^m \left[f_k(n) - \frac{g^n}{g^N} f_k(N) \right] \leqslant 0, \quad \text{(C16)}$$

so the quantity (C15) is not positive. Third, when $N < m < n$, $h_k(m) \geqslant h_k(n)$ and $g^m f_k(n) \leqslant g^n f_k(m)$, so the quantity (C15) is not positive. This completes the proof of the inequalities (C2).

Now we establish the bound (6.33) by writing the fidelity $F_0(\bar{\alpha})$ of Eq. (6.30) as

$$\begin{aligned} F_0(\bar{\alpha}) &= e^{-g^2\bar{\alpha}^2} \frac{\left[e_N(g^2\bar{\alpha}^2) + g^N \sum_{n=N+1}^{\infty} \frac{g^n \bar{\alpha}^{2n}}{n!} \right]^2}{e_N(g^2\bar{\alpha}^2) + g^{2N} \sum_{n=N+1}^{\infty} \frac{\bar{\alpha}^{2n}}{n!}} \\ &\geqslant e^{-g^2\bar{\alpha}^2} \left[e_N(g^2\bar{\alpha}^2) + g^N \sum_{n=N+1}^{\infty} \frac{g^n \bar{\alpha}^{2n}}{n!} \right] \\ &\geqslant e^{-g^2\bar{\alpha}^2} e_N(g^2\bar{\alpha}^2), \end{aligned} \quad \text{(C17)}$$

where the first inequality follows from using $g^{2N} \leqslant g^N g^n$ in the denominator. This establishes the bound (6.33).

[1] H. A. Haus and J. A. Mullen, Phys. Rev. **128**, 2407 (1962).
[2] C. M. Caves, Phys. Rev. D **26**, 1817 (1982).
[3] C. M. Caves, J. Combes, Z. Jiang, and S. Pandey, Phys. Rev. A **86**, 063802 (2012).
[4] W. K. Wootters and W. H. Zurek, Nature (London) **299**, 802 (1982).
[5] D. Dieks, Phys. Lett. A **92**, 271 (1982).
[6] E. Arthurs and J. L. Kelly, Jr., Bell Syst. Tech. J. **44**, 725 (1965).
[7] T. C. Ralph and A. P. Lund, in *Quantum Communication, Measurement and Computing*, edited by A. Lvovsky, AIP Conference Proceedings Vol. 1110 (American Institute of Physics, Melville, NY, 2009), pp. 155–160; see arXiv:0809.0326 for a slightly embellished discussion.
[8] J. Fiurášek, Phys. Rev. A **70**, 032308 (2004).
[9] A. Chefles, Phys. Lett. A **239**, 339 (1998).
[10] A. Chefles and S. M. Barnett, Phys. Lett. A **250**, 223 (1998).
[11] R. Nair, B. J. Yen, S. Guha, J. H. Shapiro, and S. Pirandola, Phys. Rev. A **86**, 022306 (2012).
[12] F. E. Becerra, J. Fan, G. Baumgartner, J. Goldhar, J. T. Kosloski, and A. Migdall, Nat. Photon. **7**, 147 (2013).
[13] The s-ordered [14] output variance is $\Sigma_s^2 = \langle \Delta a_{\rm out}^\dagger \Delta a_{\rm out} \rangle + (1-s)/2 = \mu^2(g^2-1) + (1-s)/2$.
[14] J. C. Garrison and R. Y. Chiao, *Quantum Optics* (Oxford University, Oxford, 2008).
[15] H. P. Yuen, Phys. Lett. A **113**, 405 (1986).
[16] N. Herbert, Found. Phys. **12**, 1171 (1982).
[17] N. J. Cerf and J. Fiurášek, in *Progress in Optics*, edited by E. Wolf (Elsevier, Amsterdam, 2006), Vol. 49, pp. 455–545.
[18] S. L. Braunstein and P. van Loock, Rev. Mod. Phys. **77**, 513 (2005).
[19] V. Bužek and M. Hillery, Phys. Rev. A **54**, 1844 (1996).
[20] G. Lindblad, J. Phys. A: Math. Gen. **33**, 5059 (2000).
[21] S. L. Braunstein, V. Bužek, and M. Hillery, Phys. Rev. A **63**, 052313 (2001).
[22] L.-M. Duan and G.-C. Guo, Phys. Rev. Lett. **80**, 4999 (1998).
[23] A. Chefles and S. M. Barnett, Phys. Rev. A **60**, 136 (1999).
[24] P. T. Cochrane, T. C. Ralph, and A. Dolińska, Phys. Rev. A **69**, 042313 (2004).
[25] G. Y. Xiang, T. C. Ralph, A. P. Lund, N. Walk and G. J. Pryde, Nat. Photon. **4**, 316 (2010).
[26] D. T. Pegg, L. S. Phillips, and S. M. Barnett, Phys. Rev. Lett. **81**, 1604 (1998).
[27] J. Jeffers, Phys. Rev. A **82**, 063828 (2010).
[28] F. Ferreyrol, M. Barbieri, R. Blandino, S. Fossier, R. Tualle-Brouri, and P. Grangier, Phys. Rev. Lett. **104**, 123603 (2010).
[29] F. Ferreyrol, R. Blandino, M. Barbieri, R. Tualle-Brouri, and P. Grangier, Phys. Rev. A **83**, 063801 (2011).
[30] J. Fiurášek, Phys. Rev. A **80**, 053822 (2009).
[31] P. Marek and R. Filip, Phys. Rev. A **81**, 022302 (2010).
[32] A. Zavatta, J. Fiurášek, and M. Bellini, Nat. Photon. **5**, 52 (2011).
[33] M. A. Usuga, C. R. Müller, C. Wittmann, P. Marek, R. Filip, C. Marquardt, G. Leuchs, and U. L. Andersen, Nat. Phys. **6**, 767 (2010).
[34] M. A. Usuga, Ph.D. thesis, Technical University of Denmark, 2012, http://orbit.dtu.dk/fedora/objects/orbit:112908/datastreams/file_9748178/content.
[35] C. R. Müller, C. Wittmann, P. Marek, R. Filip, C. Marquardt, G. Leuchs, and U. L. Andersen, Phys. Rev. A **86**, 010305(R) (2012).
[36] V. Dunjko and E. Andersson, Phys. Rev. A **86**, 042322 (2012).
[37] C. W. Helstrom, *Quantum Detection and Estimation Theory* (Academic, New York, 1976).
[38] H. M. Wiseman and G. J. Milburn, *Quantum Measurement and Control* (Cambridge University, Cambridge, 2010).
[39] M. Charbit, C. Bendjaballah, and C. W. Helstrom, IEEE Trans. Inf. Theory **35**, 1131 (1989).
[40] The Chernoff bound applied to the Poisson distribution $\Pr[n|\bar{\alpha}^2]$ bounds the tail probabilities in the following way:

$$\Pr[n \geqslant N|\bar{\alpha}^2] \leqslant e^{-\bar{\alpha}^2}(e\bar{\alpha}^2/N)^N, \quad \text{for } N > \bar{\alpha}^2,$$

$$\Pr[n \leqslant N|\bar{\alpha}^2] \leqslant e^{-\bar{\alpha}^2}(e\bar{\alpha}^2/N)^N, \quad \text{for } N < \bar{\alpha}^2.$$

[41] M. Abramowitz and I. A. Stegun, *Handbook of Mathematical Functions* (US Government Printing Office, Washington, 1964); formula 16.27.3. Wolfram Mathworld also denotes this function by θ_3.
[42] J. Fiurášek, Phys. Rev. A **64**, 062310 (2001).
[43] One could use symmetric ordering instead of the antinormal ordering used in these SNRs. Symmetric ordering applies when one intends to measure just one quadrature, instead of both.

[44] E. Knill, R. Laflamme, and G. J. Milburn, Nature (London) **409**, 46 (2001).
[45] J. Fiurasek and N. J. Cerf, Phys. Rev. A **86**, 060302(R) (2012).
[46] N. Walk, T. C. Ralph, T. Symul, and P. K. Lam, Phys. Rev. A **87**, 020303(R) (2013).
[47] R. W. Emerson, *Essay 2 Self-reliance*, Essays: First Series (James Munroe, Boston, 1841).
[48] The actual quote is [47]: "A foolish consistency is the hobgoblin of little minds, adored by little statesmen and philosophers and divines."